Machine learning reveals limited contribution of trans-only encoded variants to the HLA-DQ immunopeptidome by accurate and comprehensive HLA-DQ antigen presentation prediction

Jonas Birkelund Nilsson[1]*, Saghar Kaabinejadian[2,5]*, Hooman Yari[5], Bjoern Peters[4], Carolina Barra[1], Loren Gragert[3], William Hildebrand[5] and Morten Nielsen[1]

*shared first authorship

[1] Department of Health Technology, Technical University of Denmark, DK-2800 Lyngby, Denmark

[2] Pure MHC, LLC., Oklahoma City, OK, United States

[3] Department of Pathology and Laboratory Medicine, Tulane University School of Medicine, New Orleans, LA 70112, USA.

[4] Center for Infectious Disease and Vaccine Research, La Jolla Institute for Immunology, La Jolla, CA 92037, California, USA

[5] Department of Microbiology and Immunology, University of Oklahoma Health Sciences Center, Oklahoma City, OK, United States

Abstract

HLA class II antigen presentation is key for controlling and triggering T cell immune responses. HLA-DQ molecules, which are believed to play a major role in autoimmune diseases, are heterodimers that can be formed as both cis and trans variants depending on whether the α- and β-chains are encoded on the same (cis) or opposite (trans) chromosomes. So far, limited progress has been made for predicting HLA-DQ antigen presentation. In addition, the contribution of trans-only variants (i.e. variants not observed in the population as cis) in shaping the HLA-DQ immunopeptidome remains largely unresolved. Here, we seek to address these issues by integrating state-of-the-art immunoinformatics data mining models with large volumes of high-quality HLA-DQ specific MS-immunopeptidomics data. The analysis demonstrated a highly improved predictive power and molecular coverage for models trained including these novel HLA-DQ data. More importantly, investigating the role of trans-only HLA-DQ variants revealed a limited to no contribution to the overall HLA-DQ immunopeptidome. In conclusion, this study has furthered our understanding of HLA-DQ specificities and has for the first time cast light on the relative role of cis versus trans-only HLA-DQ variants in the HLA class II antigen presentation space. The developed method, NetMHCIIpan-4.2, is available at https://services.healthtech.dtu.dk/services/NetMHCIIpan-4.2.

Introduction

Major histocompatibility complex class II molecules (MHC class II) are expressed on the surface of professional antigen presenting cells such as B cells, dendritic cells (DCs), and monocytes/macrophages[1]. These molecules, which are designed to bind and present fragments of the exogenous proteins to T-helper cells, are heterodimers consisting of α- and β-chains which together form the peptide-binding cleft.

In humans, HLA (human leukocyte antigen) class II is encoded by three different loci (HLA-DR, -DQ, and -DP). These HLA genes have numerous allelic variants with polymorphisms that are mainly clustered around the peptide-binding groove, resulting in a wide range of distinct peptide-binding specificities[2]. In many autoimmune diseases, HLA class II genes are major genetic susceptibility factors[1,3] that play a central role in the pathogenesis of these conditions by presenting antigenic peptides to CD4+ T cells.

Several studies have explored the importance of HLA-DR and DQ at haplotype and genotype levels among type 1 diabetes (T1D) patients[3]. These genetic and functional studies have indicated that both HLA-DR and DQ alleles are associated with the risk of T1D[3,4]. In addition, the associated DR-DQ haplotypes demonstrate a risk hierarchy, ranging from highly predisposing to highly protective[4]. Interestingly, more recently it was demonstrated that HLA-DR, which generally plays the primary role in autoimmune diseases, has an important but secondary role to the HLA-DQ locus in T1D[5].

Autoimmune disorders like T1D in addition to other conditions such as Celiac disease, where a direct and exceptionally strong association for HLA-DQ has been established[6], thus necessitate a more thorough and systematic characterization of antigen presentation by HLA-DQ molecules to enable study of their function. Even though the field is moving forward rapidly[7], so far peptide binding motifs of only a limited number of HLA-DQ molecules have been exhaustively studied[8–10]. One reason for this is that HLA-DQ molecules are more complex to study experimentally. For instance, because of the monomorphic nature of the α-chain in HLA-DR, the polymorphic variations are only provided by the β-chain[11]**.** In HLA-DQ, both α- and β-chains contribute to polymorphic variations. However, evidence suggests that not every α- and β-chain pairing will result in a stable heterodimer due to key structural requirements on the α and β dimerization interface[11,12]. For example, DQA1*01 has only been detected to form stable heterodimers with DQB1*05 and 06 alleles. Likewise, the DQA1*02, 03, 04, 05, and 06 alleles form stable heterodimers only with the DQB1*02, 03, and 04[12–14].

In addition, studying the function of HLA-DQ alleles is challenging because of the extensive linkage disequilibrium between HLA-DR and HLA-DQ within the HLA class II region, making it difficult to differentiate the role of individual HLA-DQ alleles from the associated HLA-DR molecules[3,11].

Finally, unique *cis* and *trans* encoded DQ molecules can occur where α- and β-chains that pair to form the heterodimer are encoded by the same (*cis*) or opposite (*trans*) chromosomes, making the study of these molecules even further complicated. While the majority of the current knowledge on HLA-DQ molecules comes from cis encoded variants, the surface expression and function of a small number of trans encoded DQ variants have been confirmed[11,15]. Here, it is important to emphasize that these functional trans molecules have also been observed to be functional as the corresponding cis-encoded variant. Therefore, it is generally believed that alleles of DQα- and DQβ-chains pair up primarily in cis rather than in trans variants[16,17]. Hereafter, we refer to all stable DQα- and β-chain combinations mentioned above as cis, and the rest which includes any combination that has not been detected or reported as cis encoded will be referred to as “trans-only”.

In recent years, the information related to *cis*-encoded HLA-DQ variants has been greatly expanded due to large volumes of HLA sequence data becoming available[13]. Here, the assumption is that all observed DQ haplotypes, by natural selection, are able to form stable and functional cis and trans-encoded molecules. However, the role of trans-only encoded variants in antigen presentation and their contribution in shaping and complementing the HLA-DQ immunopeptidome has remained largely unresolved.

Given the critical role of HLA class II antigen presentation in the control and shaping of the adaptive immune response, great efforts have been dedicated to the development of prediction models capable of predicting this event (reviewed in Nielsen et al. 2020[18]). Current state-of-the-art prediction methods include NetMHCIIpan[19], a pan-specific method allowing for prediction of antigen presentation for any HLA class II molecule with known protein sequence. For HLA-DQ and DP heterodimers, this means that sequence information about both the α- and β-chains is required in order to make predictions.

Originally, in vitro peptide-HLA binding affinity (BA) assays have been used to generate data to characterize the motifs of HLA class II molecules[2], and development of different machine-learning prediction models to identify the rules of peptide–HLA binding[20,21]. However, experimental results indicate binding affinity (BA) to be a relatively weak correlate of antigen processing and presentation by HLA molecules[22]. In addition, multiple studies have demonstrated that the performance of the HLA-class II peptide-binding prediction models improve significantly when trained with immunopeptidome data acquired by liquid chromatography coupled with mass spectrometry (LC-MS/MS)[2,20,23,24]. Generally, in an HLA class II immunopeptidome eluted ligand (EL) assay, HLA molecules are affinity purified from lysed antigen presenting cells (APCs) using HLA specific monoclonal antibodies. The HLA molecules are next denatured and peptide ligands are isolated and sequenced via LC-MS/MS[25,26]. The result of such an

assay is a list of peptide sequences restricted to at least one of the HLA class II molecules expressed by the interrogated cell line. EL data has a major advantage over BA data as they contain signals from different steps of HLA class II antigen presentation, such as antigen digestion, HLA loading of ligands, and transport to the cell surface[27–29].

HLA class II binding predictions have been widely used to identify epitope candidates in infectious, cancer and autoimmune diseases[30]. The majority of prediction algorithms for HLA class II have so far been focused on HLA-DR molecules due to the large data availability for those. However, in the context of HLA-DQ, both pairing of synthetic α- and β-chains in order to perform binding affinity experiments, and generation of large EL datasets have proven to be challenging. The latter mostly due to lack of application of HLA-DQ specific antibodies in large scale MS-immunopeptidomics experiments resulting in limited yield in the HLA-DQ purification process.

In recent years, proteomics and peptide analysis by mass spectrometry (MS) has made huge progress, due to cutting edge technology and increased sensitivity of the instruments along with advanced software platforms and algorithms that support peptide identification and quantification. These advancements, along with the use of a highly specific HLA-DQ antibody, have enabled us to characterize, in a single assay, thousands of peptides which naturally bind the HLA-DQ molecules and generate stable peptide-HLA complexes that are transported to the cell surface to be presented to immune cells. Here, we have applied this setup to generate a large set of peptides presented by a group of HLA-DQ molecules frequent in the worldwide population from a panel of homozygous B lymphoblastoid cell lines. These large data sets were directly submitted to bioinformatic motif identification and machine learning pipelines to define the motifs and uncover the rules governing the processing and presentation of peptides in a biological context. Further, this study allowed us to move towards resolving the challenge of cis versus trans formation of functional HLA-DQ heterodimers and determine the role of trans-only variants in shaping the HLA-DQ immunopeptidome. The extensive insight into the peptide-binding characteristics of the investigated HLA-DQ molecules provided by this study will facilitate better understanding of HLA-DQ disease association and discovery of novel therapeutic targets.

154 # Materials and methods

155

156 ## Cell lines and antibody

157 Homozygous B lymphoblastoid cell lines (BLCL) were obtained from the International
158 Histocompatibility Working Group (IHWG) Cell and DNA bank housed at the Fred
159 Hutchinson Cancer Research Center, Seattle, WA (http://www.ihwg.org). A group of 16
160 cell lines expressing the high frequency HLA-DQ alleles were selected for the study
161 (supplementary table 1). To guarantee intact class II processing and presentation
162 machinery and to ensure that the total HLA-DQ expression represents the physiological
163 level, use of engineered cells was avoided.

164 The cells were grown in high density cultures in roller bottles in complete RPMI medium
165 (Gibco) supplemented with 15% fetal bovine serum (FBS; Gibco/Invitrogen Corp) and
166 1% 100 mM sodium pyruvate (Gibco). Cells were harvested from the suspension,
167 washed with PBS and spun down at 4C for 10 minutes. The cell pellets were
168 immediately frozen in LN2 and stored at -80 until downstream processing[23]. All cell lines
169 were subjected to high-resolution HLA typing (HLA-A, -B, -C, DRB1,3, 4, 5, DP and DQ)
170 immediately upon receipt and growth in our laboratory, for authentication prior to large
171 scale culture and data collection. The anti-human HLA-DQ specific monoclonal antibody
172 was produced in house from a hybridoma cell line (clone SPVL3) and used for affinity
173 purification of total HLA DQ from the BLCLs.

174 ## Isolation and purification of HLA-DQ bound peptides

175 HLA-DQ molecules were purified from the cells by affinity chromatography using the
176 anti-human HLA-DQ specific antibody (clone SPVL3) coupled to CNBr-activated
177 Sepharose 4 Fast Flow (Amersham Pharmacia Biotech, Orsay, France) as described
178 previously[23]. Briefly, frozen cell pellets were pulverized using Retsch Mixer Mill MM400,
179 resuspended in lysis buffer comprised of Tris pH 8.0 (50 mM), Igepal, 0.5%, NaCl (150
180 mM) and complete protease inhibitor cocktail (Roche, Mannheim, Germany). Lysates
181 were centrifuged in an Optima XPN-80 ultracentrifuge (Beckman Coulter, IN, USA) and
182 filtered supernatants were loaded on immunoaffinity columns overnight at 4C. Columns
183 were washed sequentially with a series of wash buffers[26] and were eluted with 0.2 N
184 acetic acid. The HLA was denatured, and the peptides were isolated by adding glacial
185 acetic acid and heat. The mixture of peptides and HLA-DQ was subjected to reverse
186 phase high performance liquid chromatography (RP-HPLC).

187

188 **MS**

189 **Fractionation of the HLA/Peptide Mixture by RP-HPLC**

190 RP-HPLC was used to reduce the complexity of the peptide mixture eluted from the
191 affinity column. First, the eluate was dried under vacuum using a CentriVap
192 concentrator (Labconco, Kansas City, Missouri, USA). The solid residue was dissolved
193 in 10% acetic acid and fractionated using a Paradigm MG4 instrument (Michrom
194 BioResources, Auburn, California, USA). An acetonitrile (ACN) gradient was run at pH 2
195 using a two-solvent system. Solvent A contained 2% ACN in water, and solvent B
196 contained 5% water in ACN. Both solvent A and Solvent B contained 0.1%
197 trifluoroacetic acid (TFA). The column was pre-equilibrated at 2% solvent B. Then the
198 sample was loaded at a flow rate of 120 µl/min and a two-segment gradient was run at
199 160 µl/min flow rate as described in detail in Kaabinejadian et al. 2022[23]. Fractions were
200 collected in 2 min intervals using a Gilson FC 203B fraction collector (Gilson, Middleton,
201 Wisconsin, USA), and the ultra-violet (UV) absorption profile of the eluate was recorded
202 at 215 nm wavelength.

203 **Nano LC-MS/MS Analysis**

204 Peptide-containing HPLC fractions were dried and resuspended in a solvent composed
205 of 10% acetic acid, 2% ACN and iRT peptides (Biognosys, Schlieren, Switzerland) as
206 internal standards. Fractions were applied individually to an Eksigent nanoLC 415
207 nanoscale RP-HPLC (AB Sciex, Framingham, Massachusetts, USA), including a 5-mm
208 long, 350 µm internal diameter Chrom XP C18 trap column with 3 µm particles and 120
209 Å pores, and a 15-cm-long ChromXP C18 separation column (75 µm internal diameter)
210 packed with the same medium (AB Sciex, Framingham, Massachusetts, USA). An ACN
211 gradient was run at pH 2.5 using a two-solvent system. Solvent A was 0.1% formic acid
212 in water, and solvent B was 0.1% formic acid in 95% ACN in water. The column was
213 pre-equilibrated at 2% solvent B. Samples were loaded at 5 µL/min flow rate onto the
214 trap column and run through the separation column at 300 nL/min with two linear
215 gradients: 10% to 40% B for 70 minutes, followed by 40% to 80% B for 7 minutes.

216 The column effluent was ionized using the nanospray III ion source of an AB Sciex
217 TripleTOF 5600 quadruple time-of-flight mass spectrometer (AB Sciex, Framingham,
218 MA, USA) with the source voltage set to 2,400 V. Information-dependent analysis (IDA)
219 method was used for data acquisition[23]. PeakView Software version 1.2.0.3 (AB Sciex,
220 Framingham, MA, USA) was used for data visualization.

221

Peptide Data Analysis

Peptide sequences were identified using PEAKS Studio 10.5 software (Bioinformatics Solutions, Waterloo, Canada). A database composed of SwissProt Homo sapiens (taxon identifier 9606) and iRT peptide sequences was used as the reference for database search. Variable post-translational modifications (PTM) including acetylation, deamination, pyroglutamate formation, oxidation, sodium adducts, phosphorylation, and cysteinylation were included in database search. Identified peptides were further filtered at a false discovery rate (FDR) of 1% using PEAKS decoy-fusion algorithm.

Immunopeptidome Data

The immunopeptidome data consist of MS-eluted ligand (EL) and binding affinity (BA) data from the earlier NetMHCIIpan-4.1 combined with the EL data generated specifically for this study (see above). The novel MS-immunopeptidome data set covers 14 different HLA-DQ molecules obtained from 16 homozygous BLCLs. This data was filtered as described earlier[23] to exclude potential HLA class I and other co-immunoprecipitated contaminants, resulting in a list of peptides of length 12-21.

The EL data were mapped to the human reference source proteome to define source protein context. Peptides with no identical reference match were excluded, resulting in ~4% of peptides being discarded. Finally, the EL data were enriched in a per sample-id manner with random natural peptides assigned as negatives. This enrichment was done by sampling peptides of 12-21 amino acids in length in a uniform manner in an amount equal to five times the number of peptides for the most prevalent length in the positive data for the given sample.

Our final novel data set consists of 39,334 positive and 369,313 negative peptides covering 14 unique HLA-DQ molecules. This data set is available in supplementary table 2. Merging the novel EL data with the earlier NetMHCIIpan-4.1 data (expanded to include peptides 12 amino acids in length), the complete EL data consists of 480,845 positive and 4,910,165 negative data points from 177 samples/cell lines, and the BA data consist of 129,110 data points.

The data was partitioned into five subsets for cross-validated method training and evaluation using the common-motif approach described earlier[31] merging EL and BA data ensuring that peptides sharing an identical overlap of 9 or more consecutive amino acids were placed in the same subset.

Methods

Model training

Models were trained using the NNAlign_MA machine learning framework[32] in a manner similar to that described earlier for NetMHCIIpan-4.0[2]. That is, the complete model consists of an ensemble of 100 neural networks of two different architectures both with one hidden layer and either 40 or 60 hidden neurons, with 10 random weight initializations for each of the 5 cross-validation folds (2 architectures, 10 seeds, and 5 folds). All models were trained using backpropagation with stochastic gradient descent, for 300 epochs, without early stopping, and a constant learning rate of 0.05. Only single allele (SA) data were included in the training for a burn-in period of 20 epochs. Subsequent training cycles included multi-allele (MA) data. Two main models were trained, one including the original NetMHCIIpan-4.1 data and one including the novel HLA-DQ data. Furthermore, an additional model was trained with the novel data using peptide context encoding. Here, context was defined in both the peptide's N- and C-terminal as three residues from the source protein flanking the peptide, along with three starting residues from the peptide, all concatenated into a 12-mer amino acid sequence. For further details refer to Barra et al. 2018[27].

Performance evaluation and MHC restriction deconvolution

HLA annotation for MA datasets is based on which HLA molecule expressed in a given cell line has the highest prediction score for a given ligand. To balance the differences in the prediction score distributions between HLAs, percentile normalized prediction scores for each molecule were generated by ranking against a distribution of prediction scores of random natural peptides as described earlier[19,33].

Performance was evaluated on the concatenated cross-validation test set predictions using three separate metrics, namely AUC (Area Under the ROC Curve), AUC 0.1 (Area Under the ROC Curve integrated up to a False Positive Rate of 10%) and Positive Predictive Value (PPV). Each metric was calculated in a per-HLA manner from the "raw" prediction scores after HLA annotation. Further, the PPV was calculated as the fraction of true positives in the top N predictions, where N is the number of ligands assigned to a given HLA molecule. For the per-HLA performance evaluation, only HLA molecules with at least 10 positive peptides in both models were included in the performance evaluation, to ensure a level of certainty in the calculated performance metrics.

Statistical tests

Statistical tests in the performance evaluation were performed using one-tailed binomial tests excluding ties, with a significance level of 0.05. The alternative hypothesis in these tests is thus that the model trained with the novel data is more likely to perform better on a given HLA molecule than the model trained without.

Consistency correlation matrix analysis

In order to assess the novel DQ data's impact on NNAlign_MA's motif deconvolution, a consistency correlation matrix analysis was performed as described earlier[2]. To avoid potential MS co-immunoprecipitated contaminant peptides biasing this analysis, the union of identified trash peptides (i.e. positive peptides given a percentile rank greater than 20 in either of the two models) was removed. A position-specific scoring matrix (PSSM) was next generated for each molecule in each cell line based on the predicted peptide binding cores. Here, a minimum of 20 positive peptides was required in order for a PSSM to be generated. Then, for each pair of cell lines sharing a given molecule, the Pearson Correlation Coefficient (PCC) between the molecule's PSSMs was calculated. The mean consistency value for a given molecule was then given as the average PCC over each unique cell line pair (excluding self-correlations). This metric thus indicates how consistent the identified binding motifs are across different datasets for each HLA class II molecule.

Similarity distance measure

Distance between two HLA class II molecules was estimated as described earlier[34] from the pseudo-distance of the two molecules, i.e.

$$d = 1 - \frac{s(A,B)}{\sqrt{s(A,A) * s(B,B)}}$$

where s(X,Y) is the summed BLOSUM 50 similarity between the pseudo-sequences of molecule X and Y. Here, the pseudo-sequences are defined as described earlier from the set of 34 polymorphic residues within the HLA sequence concatenated into a continuous sequence, of which 15 and 19 residues derive from the α- and β-chain, respectively[35].

Estimation of prevalent stable HLA-DQ molecules

A list of HLA-DQ α- and β-chains forming prevalent stable HLA-DQ heterodimers was constructed by first obtaining lists of DQA1 and DQB1 alleles with annotated worldwide allele frequencies. This was done by querying the allelefrequencies.net database[36] for high resolution alleles in populations of size 100 and above. Next, worldwide allele frequencies were obtained as population size weighted averages capping the maximum population size to 1000. Finally, a list of prevalent HLA-DQ molecules was constructed by pairing all α and β combinations following the restrictions outlined in table 1, only including molecules with a combined allele frequency greater than 0.00005. This resulted in a list of 154 HLA-DQ molecules.

DQA1* - DQB1*	DQA1* - DQB1*
DQA1*01-DQB1*05	DQA1*04-DQB1*02
DQA1*01-DQB1*06	DQA1*04-DQB1*03
DQA1*02-DQB1*02	DQA1*04-DQB1*04
DQA1*02-DQB1*03	DQA1*05-DQB1*02
DQA1*02-DQB1*04	DQA1*05-DQB1*03
DQA1*03-DQB1*02	DQA1*05-DQB1*04
DQA1*03-DQB1*03	DQA1*06-DQB1*02
DQA1*03-DQB1*04	DQA1*06-DQB1*03
	DQA1*06-DQB1*04

Table 1: List of DQA1-DQB1 haplotypes extracted from Creary *et al.* and Petersdorf *et al.*[13,14]. Due to the relatively small sample size for some populations included in the study by Creary et al., the reported alleles and haplotypes may not reflect all haplotypes observed in the entire populations. Therefore, in this table only low-resolution (2 digit) DQ haplotypes were included to define the observed DQA1-DQB1 haplotypes.

Estimation of worldwide haplotype frequencies

Worldwide HLA-DQ haplotype frequencies were estimated by querying the allelefrequencies.net database[36] for high resolution DQ haplotypes in populations of size 100 and above, average across population as described above for HLA-DQ frequencies.

HLA-DQ specificity trees

An HLA-DQ specificity tree was constructed by first reducing the list of 154 prevalent HLA-DQ molecules to the set of unique pseudo-sequences among the molecules. Then, each unique pseudo-sequence was mapped to a representative HLA-DQ molecule name. By default, a DQ molecule in the list of molecules covered by the training data was used to represent a pseudo-sequence when possible. Furthermore, all 14 DQ molecules in the novel data were used to represent their given pseudo-sequences. In other cases of multiple options for a given pseudo-sequence, the most prevalent DQ molecule in terms of global allelic frequency was chosen. The specificity tree was then calculated using the MHCCluster method[37] and visualized using the Iroki phylogenetic tree viewer[38].

A similar tree was constructed based on clustering of the DQ pseudo-sequences. This tree was calculated with ClustalW-2.1[39] using its phylogenetic tree function, and again visualized using the Iroki tree viewer[38].

365

366 *Independent benchmark*

367 For our benchmark against MixMHC2pred-2.0[7], an independent dataset was taken from
368 Marcu et al.[40], which consists of eluted ligand data from 17 donor samples. This data
369 was enriched with random negative peptides similarly to the training data. To reduce
370 bias, peptides which were present in the EL training data of our method were not
371 included in the benchmark. This yielded a total of 165,650 positive and 2,952,352
372 negative peptides covering 71 HLA class II molecules.

373

374 Performance was evaluated on a per-sample basis in terms of AUC, AUC 0.1, and PPV.
375 For both our method and MixMHC2pred, the HLA annotation for each peptide was
376 based on the lowest reported percentile rank scores for the HLA molecules in the given
377 sample. Furthermore, as MixMHC2pred recommends using its reported percentile rank
378 scores for all analyses, its predictive performance was calculated using these rank
379 scores.

380

381

382

Results

For the study, immunopeptidome data for 14 different HLA-DQ molecules was obtained from 16 homozygous B Lymphoblastoid Cell Lines (BLCLs) using LC-MS/MS. By using a DQ-specific antibody during the affinity purification, we were able to obtain a large dataset highly enriched in DQ peptide ligands. An overview of the cell lines' peptide counts, DQ HLA types and peptide length distributions is shown in figure 1. Overall, the data contains a total of 39,334 peptide ligands, with 14- and 15-mers being most prevalent. After enriching the novel data with random natural peptides assigned as negatives (see materials and methods), we combined it with the data used to train the NetMHCIIpan-4.1 prediction method, yielding a large dataset of eluted HLA class II ligands. From this, we set out to address three essential issues related to HLA-DQ, namely i) the relatively low predictive power of current prediction models for DQ molecules, ii) the contribution of trans-only encoded DQ variants to the DQ immunopeptidome, and iii) the overall coverage of the DQ specificity space of the current experimental data and developed in-silico prediction models.

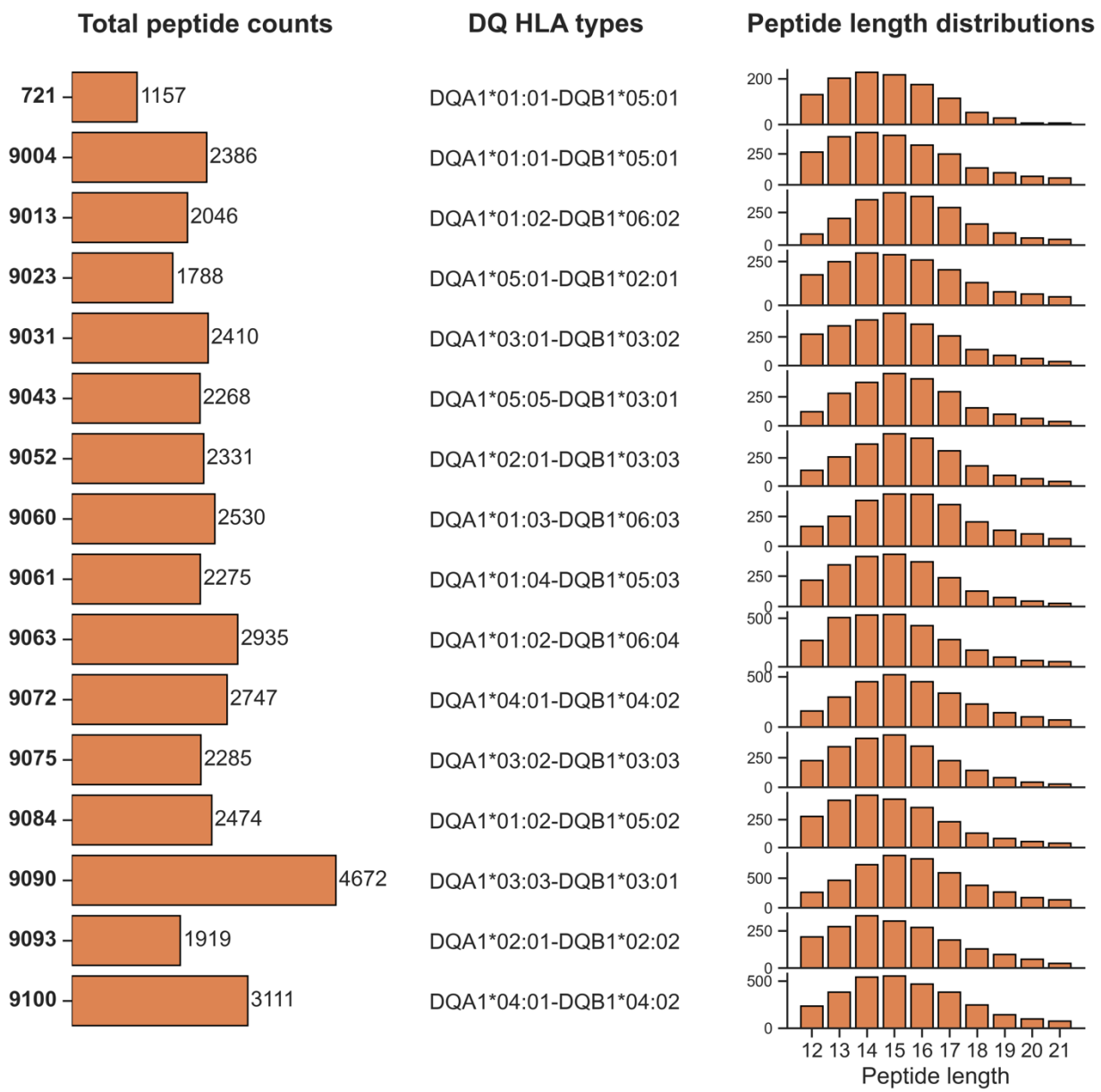

Figure 1: Overview of the novel immunopeptidomics data. Each row corresponds to a dataset from a given DQ-homozygous cell line. **Left panel**: Bar plot of overall peptide counts. The numbers on the left correspond to the cell line IDs. **Middle panel:** DQ HLA types of the cell lines. **Right panel**: Peptide length distributions.

Impact of novel DQ data on predictive performance

To investigate the impact on the predictive power by integration of the novel DQ data, we employed the NNAlign_MA algorithm[32] which is a highly powerful machine learning method for deconvoluting MS immunopeptidomics data. Two peptide antigen presentation prediction models were trained: one including the novel DQ affinity purified data (termed w_Saghar_DQ), and for direct comparison of the impact of the novel data one without (termed wo_Saghar_DQ). The models were then evaluated using cross-validation on a per-molecule basis within four different subsets of all the HLA class II molecules in the training data. These subsets are non-DQ molecules (NotDQ), all DQ molecules (DQ), DQ molecules present in the novel data (DQ_Saghar) and DQ molecules not present in the novel data (DQ_NotSaghar).

Figure 2 displays the result of this experiment and demonstrates that incorporation of the novel DQ data resulted in a significant performance gain for DQ as expected ($p=0.011$ for all metrics, one-tailed binomial test without ties). However, from these results it is apparent that the performance for DQ remains lower compared to that of non-DQ molecules. We assumed this to be a result of the DQ performance being calculated from a mix of both the novel data and the older NetMHCIIpan-4.1 training data. To demonstrate this, we evaluated the performance of the DQ_Saghar molecules limited to the novel data only. The result of this is shown in figure 3 and demonstrates that when focusing only on the novel data, the performance of DQ reaches a level comparable to that of non-DQ (median AUC values for DQ_Saghar and NotDQ are 0.9303 and 0.9312, respectively). This result is important as it suggests that the low performance earlier reported for DQ is at least in part imposed by a low quality and quantity of the earlier DQ data.

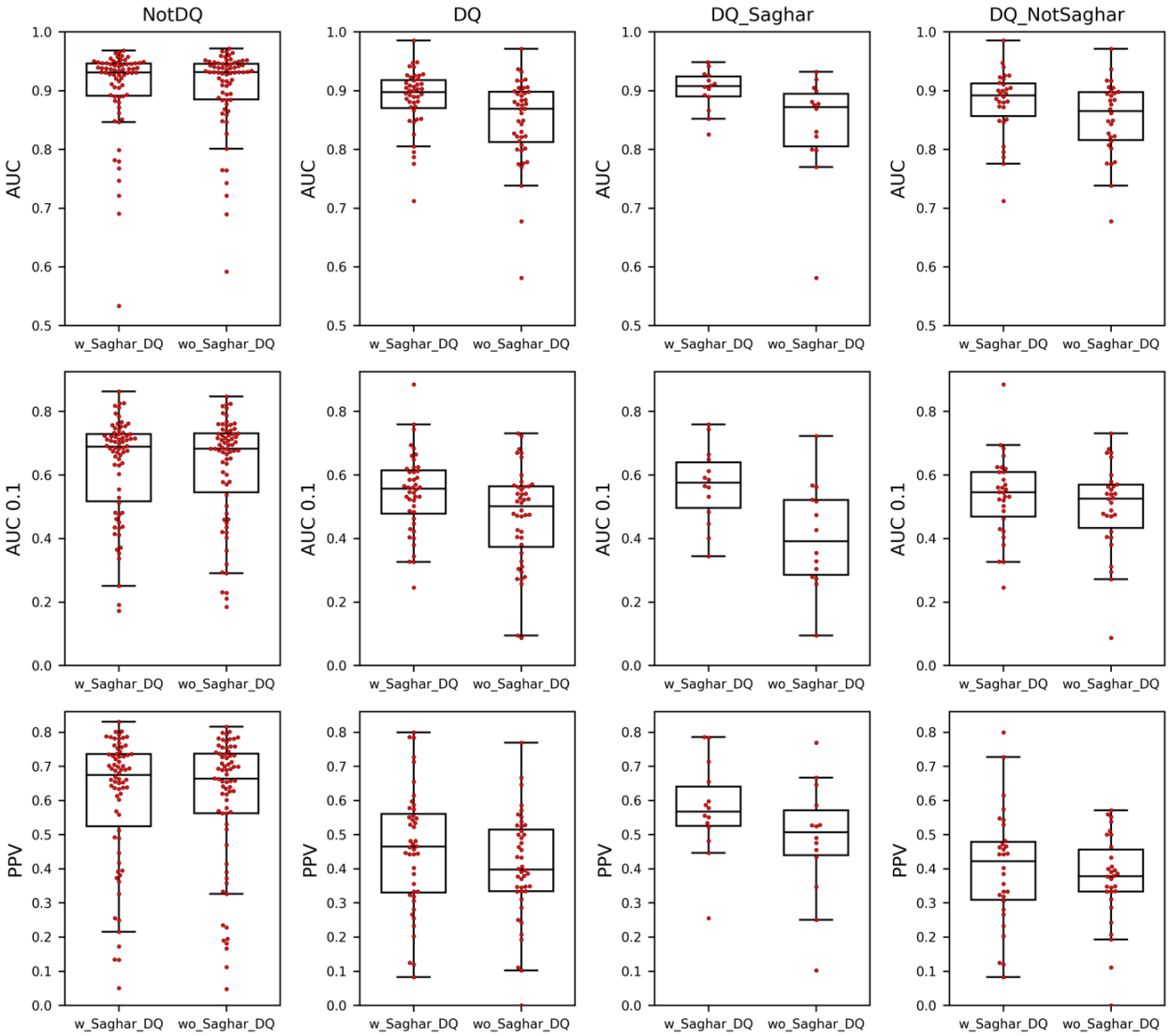

Figure 2: AUC, AUC 0.1 and PPV predictive performance for the models trained with (w_Saghar_DQ) and without (wo_Saghar_DQ) the novel data. Each point is the performance metric for a unique HLA class II molecule. For details on the performance metrics refer to materials and methods. The columns correspond to four different subsets of HLA molecules, namely all non-HLA-DQ molecules (NotDQ), all DQ molecules (DQ), DQ molecules in the novel data set (DQ_Saghar), and DQ molecules not present in the novel data (DQ_NotSaghar).

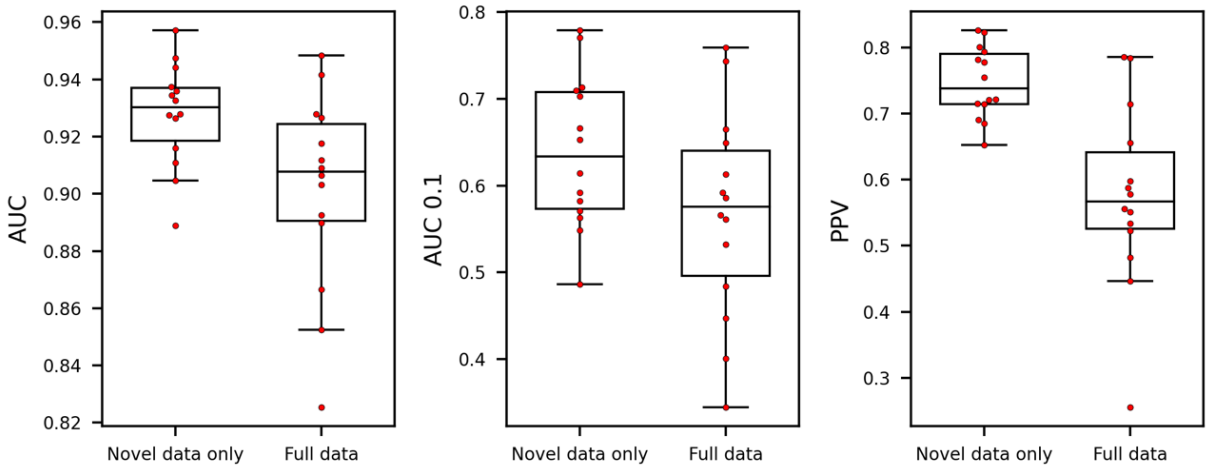

Figure 3: Performance of model trained including the novel data, evaluated on both the novel data alone, as well as the full dataset. Each point is the performance metric for an HLA-DQ molecule present in the novel data.

We next looked at the differences in peptides assigned to HLA-DQ molecules between the two methods across all samples. Here, we considered all peptides which were assigned to DQ with percentile rank less than 20 (i.e. as non-trash) in at least one of the methods[23]. Overall, the two methods share a high degree of overlap in the peptides assigned to DQ (60,959 annotations were shared by both models, 9309 annotations were unique for the method trained including the novel data and 4316 unique for the method trained without). This increased DQ coverage for the model trained including the novel data predominantly comes from peptides assigned to DR (and to some degree trash and DP) by the model trained without the novel data (see supplementary table 3 for an overview of the peptide migrations). This suggests that at least part of the improved predictive performance of the novel model originates from an improved motif deconvolution.

To further quantify this, we show the mean consistency value per HLA molecule in the four molecule subsets in supplementary figure 1. In short, position-specific scoring matrices were constructed for each molecule in a given cell line from the predicted binding cores in the individual positive peptides, and the consistency was quantified by the correlation of such matrices for the same molecule between different cell line data sets (for details refer to materials and methods). Based on this analysis, an overall improved consistency is observed for the model trained with the novel DQ data ($p<0.02$ in all cases except for the DQ_NotSaghar subset, one-tailed binomial test without ties). The consistency analysis for an example molecule contained in the novel data (DQA1*03:01-DQB1*03:02) is shown in supplementary figure 2, illustrating that in most cases the improved motif consistency is caused by an increased peptide count across samples (see supplementary tables 4 and 5).

Furthermore, HLA-DQ binding motifs obtained by motif deconvolution of the novel MS data were visualized, along with sequence motifs based on predicted binders, in supplementary figure 3. Here, the logos obtained by motif deconvolution are in most cases very similar when comparing the models trained with and without the novel data. However, the predicted sequence logos based on top scoring random natural peptides indicate that the model trained without the novel DQ data has failed to fully learn the correct binding motifs of all the novel DQ molecules, especially with respect to the P1 amino acid preferences. To quantify these results, correlations between the deconvoluted and predicted logos for each method were calculated (supplementary figure 4). This analysis showed significantly higher correlation for the method including the novel data ($p=0.011$, one-tailed binomial test without ties), indicating a highly consistent correspondence between the identified and predicted binding motifs.

Together, these observations demonstrate that incorporating the novel HLA-DQ data has allowed for an enriched identification of HLA-DQ peptide ligands, rescuing peptides otherwise assigned to alternative DR/DP molecules, resulting in improved motif deconvolution consistency and improved predictive power.

The above results were complemented by a comparison to a model trained including the novel data using peptide context encoding. In short, context encoding refers to a scenario where information from the regions flanking the peptide is extracted from the source protein sequence and included as additional input to the machine learning model. In line with what has been demonstrated earlier[2,27,32], the results of this comparison (supplementary figure 5) demonstrated that the model trained including context significantly outperformed the model trained without context in all performance metrics and data subsets (the only exception being the DQ_NotSaghar subset). However, given that the main focus of the remaining part of the manuscript is to investigate motif deconvolution and the role of cis versus trans-only DQ α- and β-chain pairing in this context, we focus on the simpler model trained without context information from here on.

507
508 **Distribution of annotations to cis vs trans-only DQ molecules**
509
510 In DQ-heterozygous cell lines, four possible α-β chain pairings can in principle be
511 observed. For so-called cis-heterodimers, the α- and β-chain are expressed on the
512 same chromosome and can thus be observed in haplotype sequencing. DQ molecules
513 formed by pairing α- and β-chains between chromosomes are called trans-
514 heterodimers. Some α-β pairings have not been observed as cis encoded (based on
515 large HLA-haplotype sequencing population studies) and are thus here referred to as
516 "trans-only" combinations. To assess the relative contribution of cis and trans-only DQ
517 heterodimers in shaping the immunopeptidome, we investigated the distribution of
518 peptides assigned to cis versus trans-only encoded DQ molecules across DQ-
519 heterozygous datasets for the two models. Here, only datasets with at least 100 DQ-
520 annotated peptides excluding trash in both methods were considered (for an overview
521 of the datasets used in this analysis, refer to supplementary table 6). The proportion of
522 DQ-annotated peptides assigned to each molecule was then calculated for each dataset
523 containing that molecule. Finally, the mean per-dataset peptide fraction was reported for
524 each DQ molecule, and the distribution of these means for molecules across four
525 categories were then investigated. These categories are all cis variants, cis-SA (cis
526 variants part of the DQ-SA training data), cis-MA (cis variants part of the DQ-MA
527 training data), and trans-only variants.
528
529 The result of this analysis is shown in figure 4A for the two models and indicates that for
530 the method including the novel data, trans-only molecules consistently cover a small
531 proportion of the DQ annotations in each cell line. On the other hand, the cis molecules
532 have generally high contribution, with the cis-SA molecules having the largest
533 contribution as expected. However, the cis-MA molecules were also found to have
534 significantly larger contribution than the trans-only molecules in the model including the
535 novel data ($p=0.005$, two-sample t-test). Similar results were found when extending the
536 cis-SA category to include cis-MA molecules with the same pseudo-sequence as a cis-
537 SA molecule (supplementary figure 6). Further, an overall higher contribution of trans-
538 only molecules to the DQ peptide annotations was observed for the model trained
539 without the novel data ($p=0.03$, paired one-sided t-test). These results are striking, as
540 they indicate that the motif deconvolution in the model including the novel data is not
541 solely driven by the cis-SA molecules, but rather by an overall preference for cis-
542 encoded variants compared to trans-only variants (see supplementary figures 7 and 8).
543
544 To further investigate this, the DQ motif deconvolution of the two models for the
545 Racle__TIL1 dataset is shown in figure 4B. Here, the model trained without the novel
546 data assigns a large proportion of peptides (170 out of 425) to HLA-DQA1*01:01-

547 DQB1*03:01, which is a trans-only molecule known to not form a stable
548 heterodimer[12,13]. On the other hand, in the model trained with the novel data, almost no
549 peptides are assigned to this molecule (20 out of 459). Instead, the peptides are
550 assigned to the cis molecule HLA-DQA1*03:03-DQB1*03:01. Note, also, that for both
551 models a very minor proportion of peptides are assigned to HLA-DQA1*03:03-
552 DQB1*05:01, another trans-only heterodimer known to be unstable[12,13]. Overall, these
553 results demonstrate that the model including the novel DQ data allows for proper motif
554 deconvolution with limited assignment of peptides to trans-only HLA-DQ molecules.
555 Further, the very low proportion of peptides assigned to trans-only molecules, combined
556 with the overall increased HLA-DQ peptide volume and motif consistency of the model
557 trained including the novel data, strongly suggests that trans-only HLA-DQ molecules
558 are unstable, non-functional and have limited to no contribution to the total HLA-DQ
559 immunopeptidome.

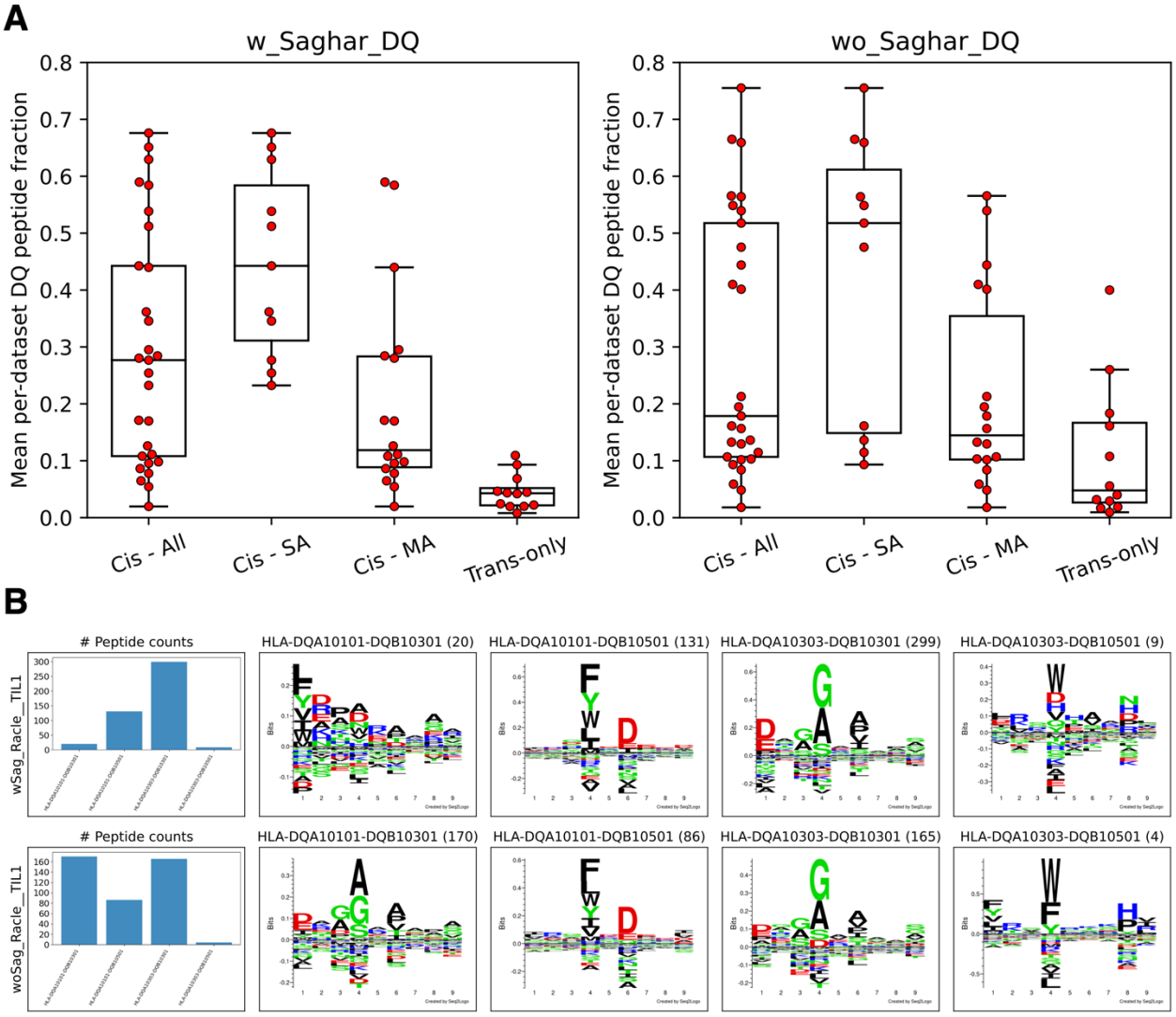

Figure 4: Contribution of cis and trans-only DQ variants in DQ-heterozygous datasets. A: Peptide-count contribution of cis and trans-only molecules in the methods with (w_Saghar_DQ) and without (wo_Saghar_DQ) the novel data. Each point shows the mean per-dataset peptide fraction for a given DQ molecule. The cis molecules are shown in three categories, namely all cis molecules (Cis - All), cis molecules found in the DQ-SA training data (Cis - SA), and cis molecules only found in the DQ-MA training data (Cis - MA). **B:** DQ motif deconvolution for the Racle__TIL1 dataset**.** The rows correspond to the methods trained with (wSag) and without (woSag) the novel data, respectively. Peptide counts (excluding trash peptides) are displayed in parenthesis in the logo plot titles.

570
571 **Difference in peptide length distributions of DR and DQ**
572 When we compared the length distribution of DQ peptide ligands in the novel data with
573 HLA-DR restricted peptides that were purified from the same set of BLCLs[23], it was
574 revealed that the DQ ligands were in general shorter than the DR ligands (see
575 supplementary figure 9). By comparing the per-molecule median peptide lengths for the
576 two loci, a significant difference was found ($p<0.03$, two-sample t-test), with DR and DQ
577 having average peptide length medians of 15.41 and 14.93, respectively. This analysis
578 indicates that HLA-DQ molecules generally bind shorter peptides compared to HLA-DR.
579 Moreover, in contrast to HLA-DQ alleles that are more consistent in their peptide length
580 preferences, various HLA-DR molecules show subtle differences in their length
581 preferences[23]. For example, HLA-DR*07:01, 09:01 and 14:01 show a preference for
582 shorter peptides (14 mers) while the majority of DR alleles follow the common class II
583 length preference (15 mer).
584
585
586 **Coverage of DQ**
587 Next, we wanted to assess the number of DQ molecules present in the cross-validation
588 predictions by each model which were properly covered (i.e. had a large number of
589 peptides assigned during training), and hence where the models are expected to
590 achieve accurate predictive power. The peptide count for a given DQ molecule was
591 estimated as the accumulated sum of peptides from each cell line containing that
592 molecule (excluding trash peptides). Here, only peptides annotated to DQ molecules in
593 a given cell line corresponding to at least 5% of the total number of DQ peptides were
594 included in its count (this was done to avoid including accumulation of low count noise).
595 A given DQ molecule was then said to be covered if the summed peptide count over all
596 cell lines was at least 100. This analysis resulted in 24 DQ molecules being covered by
597 the model trained including the novel data, and 23 being covered when excluding these
598 data. None of the 24 DQ molecules covered by the model including the novel data were
599 found to be trans-only, whereas the model without the novel data covered two trans-
600 only DQ molecules, namely HLA-DQA1*01:01-DQB1*03:01 (as described earlier) and
601 HLA-DQA1*01:03-DQB1*03:02. Of the remaining 21 molecules, 20 were included in the
602 molecules covered by the model trained with the novel data.
603
604 Given the different sets of molecules covered by the two methods, we wanted to
605 estimate each method's coverage when considering the entire DQ specificity space. As
606 such, for each of the two methods, we investigated the proportion of 154 prevalent DQ
607 molecules that had a distance of at most 0.025 to a molecule covered by the model (this
608 set of molecules is here referred to as 'extended coverage'). For details on how this
609 distance was determined and how the list of prevalent DQ molecules was defined refer

610 to materials and methods. The threshold of 0.025 was chosen based on the distance at
611 which the model trained without the novel data could reach optimal performance on
612 molecules not part of the method's DQ-SA training data (see supplementary figure 10).
613 Note, also, that 0.025 is a conservative distance threshold, and that we expect the
614 model to maintain accuracy also for molecules falling beyond this value[35].
615
616 From this analysis, a significant gain in extended coverage was found (p=0.027, chi-
617 squared test), with the model including the novel data covering 94 out of 154 molecules,
618 while the model without the novel data only covered 75 out of 154 molecules (see
619 supplementary tables 7 and 8 for a list of covered and non-covered DQ molecules for
620 the model trained including the novel data). When comparing the covered and non-
621 covered molecules for the method including the novel data, the non-covered group had
622 significantly lower worldwide haplotype frequency data as obtained from
623 Allelefrequencies.net (for detail on how these frequencies were obtained refer to
624 material and methods) compared to the covered group (average frequencies for the two
625 groups were 0.0134 and 0.0025, p<0.03, student t-test). These results suggest that the
626 non-covered DQ molecules are of limited importance seen from a population coverage
627 perspective.
628
629 For visualizing the coverage of the DQ space, a specificity tree was constructed. Here,
630 we used the list of 154 prevalent HLA-DQ molecules as the starting point. This list was
631 first reduced to a set of 61 molecules with unique specificities (for details see methods)
632 which were included in the subsequent analysis. Next, a specificity tree was constructed
633 covering the 61 DQ molecules applying the MHCCluster method[37]. In short, the
634 MHCCluster method estimates the similarity between two MHC molecules using the
635 correlation between predicted binding values for a large set of random natural peptides.
636 Figure 5 shows the resulting specificity tree along with predicted binding motifs for the
637 14 novel DQ molecules. The tree displays wide coverage of the DQ space, as all the
638 novel molecules are spread more or less uniformly across the different branches of the
639 tree, and all branches are covered by one or more DQ molecules in close distance to
640 the DQ molecules covered by the training data. Moreover, a few subclusters of non-
641 covered molecules were observed (highlighted by motifs in red frames), which were
642 found to correspond almost one-to-one with the non-covered clusters in a phylogenetic
643 tree of the DQ pseudo-sequences (see supplementary figure 11).
644

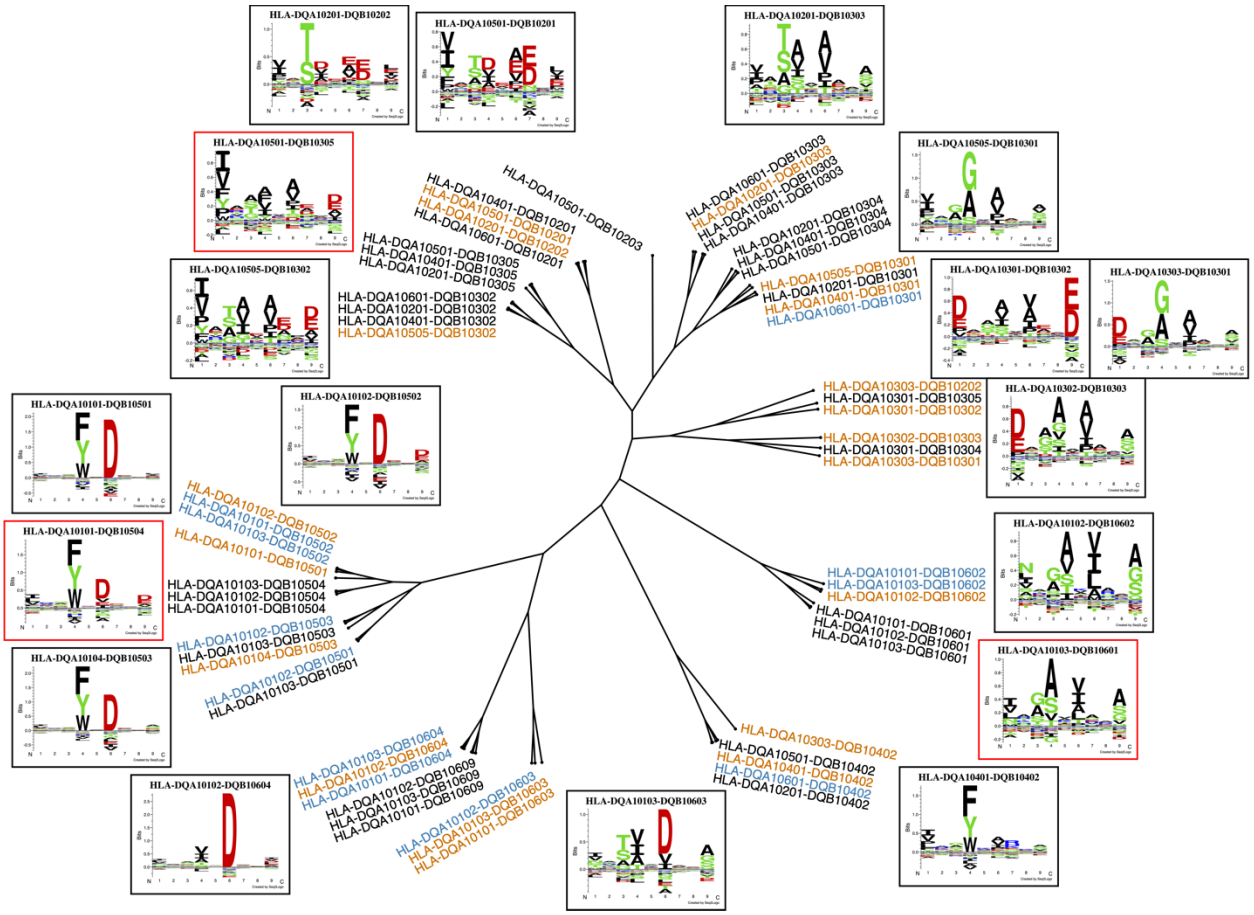

Figure 5: HLA-DQ specificity tree. The tree is based on 61 DQ molecules including the 14 molecules described by the novel data. Orange molecules are covered by the method including the novel data with at least 100 peptides, and blue molecules are within a distance 0.025 of an orange molecule. Black molecules are non-covered (i.e. have peptide count less than 100 and have distance greater than 0.025 to an orange molecule). Logos in black frames correspond to orange molecules. Logos in red frames correspond to molecules from branches with clusters of non-covered (black) molecules. The specificity tree was calculated from the pairwise similarities between the predictions scores for the DQ molecules for a set of 100,000 random natural 13-17mer peptides. Logos were constructed for the top 1% highest scoring binding cores for these 100,000 peptides.

NetMHCIIpan-4.2

The model developed here including the novel DQ immunopeptidome data is made publicly available at https://services.healthtech.dtu.dk/service.php?NetMHCIIpan-4.2. The method allows for prediction of HLA antigen presentation to all HLA-DQ molecules, and prediction can be made with or without context encoding.

660

661 **Benchmark on independent DQ data**

662 As a final showcase of our method's motif deconvolution power for DQ, we
663 benchmarked our method against MixMHC2pred-2.0, another HLA class II predictor
664 which was recently published[7]. The benchmark data was taken from Marcu et al.[40] and
665 consists of eluted ligand data from 17 donor samples, which was enriched with random
666 negative peptides.
667
668 Figure 6A shows the performance of the two methods per sample on the entire data,
669 indicating that our method significantly outperforms MixMHC2pred on the independent
670 dataset in all three metrics ($p<0.05$ in all metrics, one-tailed binomial test without ties).
671 Furthermore, figure 6B shows the performance per sample restricted to the union of
672 peptides annotated towards DQ by either method, once again showing significant
673 performance gain in favor of NetMHCIIpan-4.2 ($p<0.01$ in all metrics, one-tailed binomial
674 test without ties). It should be noted that both methods identified a large proportion of
675 trash peptides with percentile ranks greater than 20 in the data (~21% and ~32% for
676 NetMHCIIpan-4.2 and MixMHC2pred, respectively). This suggests a poor data quality in
677 general, yielding substantially lower performance than observed in our cross-validation.
678 However, the overall performance gain of our method compared to MixMHC2pred
679 suggests that NetMHCIIpan-4.2 is more powerful in the motif deconvolution and
680 identification of DQ ligands.
681
682 Investigating our method's motif deconvolution on the DQ-heterozygous samples, we
683 observed that the trans-only molecules once again had limited to no contribution (see
684 supplementary figure 12A). In terms of observed cis variants found in the DQ-SA or DQ-
685 MA training data (cis-SA and cis-MA, respectively), the cis-SA molecules had the
686 largest contribution as expected, with cis-MA having significantly larger contribution than
687 the trans-only variants ($p=0.0002$, two-sample t-test). Similar results were found when
688 taking into account cis-MA molecules with the same pseudo-sequence as a cis-SA
689 molecule (supplementary figure 12B). This result contrasts with what was observed for
690 MixMHC2pred, where close to an equal contribution was observed across the different
691 molecule classes. Furthermore, when examining the motif deconvolution of the DQ-
692 heterozygous samples without trans-only molecules, our method was able to identify
693 four distinct motifs in each sample (see supplementary figure 12C).

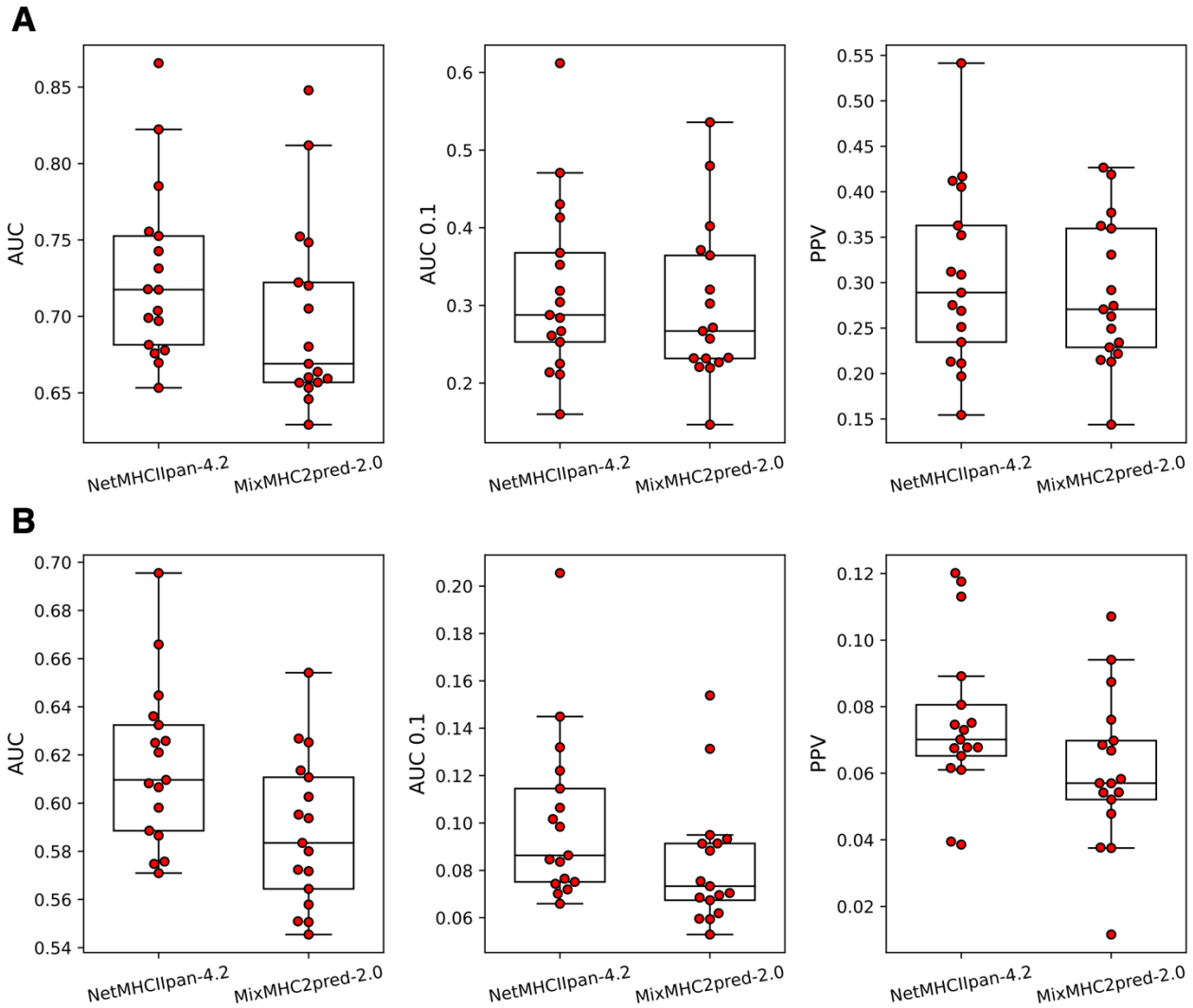

Figure 6: Benchmark against MixMHC2pred-2.0 in terms of AUC, AUC 0.1 and PPV. A: Performance per sample calculated on the entire data. **B**: Performance per sample calculated on the union of DQ-annotated peptides between the two methods.

Discussion

In this work, we have demonstrated how rational data generation combined with refined immunoinformatics data mining can boost the performance of HLA class II antigen presentation predictions and move towards closing the performance gap between HLA-DR and HLA-DQ.

We generated high quality MS-immunopeptidomics data from a series of 16 HLA-DQ homozygous cell lines covering a total of 14 frequent HLA-DQ molecules in different populations worldwide. Using an in-house HLA-DQ specific antibody enabled identification of MS-immunopeptidomics datasets of an, in a DQ context, unprecedented volume with an average of 2,600 unique peptides identified in each cell line. Integrating this large volume of data with earlier data from the development of NetMHCIIpan-4.1 allowed us to boost the HLA-DQ antigen presentation predictive performance to a level comparable to that of HLA-DR. Investigating the accuracy of the motif deconvolution of the two methods trained with and without the novel data demonstrated an overall improved motif consistency across all HLA molecules. This observation demonstrates how integration of the novel HLA-DQ data results in an overall improved HLA-restriction assignment of the individual MS-HLA-peptides leading to more accurate motif characterizations across all three HLA class II loci. The main source of this improvement was demonstrated to be an increased volume of peptide assignment to HLA-DQ molecules during the motif deconvolution. This resulted in improved motif accuracy for both HLA-DQ imposed by the larger volume of peptides, and non HLA-DQ molecules by the removal of peptides mis-assigned as DQ restricted by the model not including the novel DQ data.

Next, moving into the issue of cis versus trans-only HLA-DQ α- and β-chain combinations, we demonstrated that in contrast to the method without the novel data, the model trained including the novel data performed the DQ motif deconvolution almost solely using known HLA-DQ cis-variants. One particular example here was the HLA-DQ molecule DQA1*01:01-DQB1*03:01, which was assigned a large number of peptides in the model trained without the novel data. However, when including the novel data, the peptide assignment to this molecule was almost completely depleted. This result combined with the overall increased HLA-DQ peptide volume and motif consistency of the model trained including the novel data, strongly suggests that trans-only HLA-DQ α and β combinations are non-functional and have minimal or no contribution to the total HLA-DQ immunopeptidome. This finding is striking since the definition of cis and trans-only dimerization defined here precisely follows the rules proposed earlier for forming

stable/unstable HLA-DQ heterodimers. Specifically, the rules indicate that structural constraints do not favor dimerization of DQA1*01 with DQB1*02, 03, and 04 alleles, resulting in their inefficient assembly, lack of stability and surface expression and therefore loss of function[12,14]. These results thus demonstrate how such rules can be learned directly from MS-immunopeptidome data using tailored data mining methods and rationally defined data sets, suggesting that similar types of analysis should be extended to HLA-DP to further our understanding of cis versus trans α- and β-chain pairing.

Note, that the definition of cis and trans-only HLA-DQ α- and β-chain combinations applied in this work is contingent on the current haplotype data available and the assumption that all observed haplotype α and β combinations can pair and form cis-variants, and all other combinations not observed as such cis-variants are trans-only. The current data defining these categories are limited in volume, and larger sample sizes are required for more accurate analyses particularly for the more heterogeneous groups and low frequency haplotypes[13].

Lastly, we demonstrated how the coverage of HLA-DQ molecules was largely increased by the models trained with the novel data and illustrated this by constructing an HLA-DQ tree showing coverage of all branches. This suggests that the current model covers all HLA-DQ binding specificities (considering that *trans-only* HLA-DQ molecules have limited to no contribution to the overall HLA-DQ immunopeptidome).

Overall, this work has demonstrated how careful data generation using a DQ-specific antibody and affinity purification combined with refined data mining and motif deconvolution can be applied towards closing the performance gap in peptide binding prediction between HLA-DR and HLA-DQ. Despite the large performance gain demonstrated here, the accuracy for HLA-DQ remains below what is observed for DR. We demonstrate that this to a very large degree can be attributed to the generally lower quantity and quality of ligands obtained in earlier DQ immunoprecipitation studies where most often DQ (and DP) data have been obtained using a pan-HLA class II antibody (after first depleting for HLA-DR[29]). Focusing solely on the novel data generated in this study, we find that both the quantity and quality of the obtained DQ ligands are on par with what is found for HLA-DR, resulting in predictive performance for the associated dataset being equal between the two. This result has large impacts and suggests that modeling DQ is a task of equal complexity to that of HLA-DR, and that the current lower performance of DQ compared to DR is driven by low quantity and quality of data; a situation that can be resolved by generation of high quality and volume data as outlined in this study.

In conclusion, other than demonstrating an overall improved predictive performance and coverage of HLA-DQ molecules, a key result of our work is an improved understanding of the relative contribution of cis versus trans-only paired molecules to the total HLA-DQ immunopeptidome demonstrating a very limited role of the latter in complementing the specificity space. We believe these findings will provide a foundation for further research defining the molecular role of HLA-DQ in the onset of cellular immunity within autoimmune and infectious diseases.

Acknowledgements

We would like to sincerely thank Dr. Rico Buchli (Pure Protein, LLC) for providing the SPVL3 affinity columns for this study. We also thank Steven Cate (University of Oklahoma Health Sciences Center) and Sean Osborn (Pure MHC, LLC) for HLA typing of the BLCLs and very helpful discussions.

Author contributions

SK and MN designed the study. The experimental data used in the study was generated by SK, with contribution from HY and WH. JN and MN generated the computational results and figures. CB, LG and BP contributed towards methodology and provided scientific feedback. The manuscript was written by JN, SK and MN, with contributions from all authors. All authors have read and approved the final version of the paper.

Competing interests

SK is an employee at Pure MHC, LLC. The remaining authors declare no competing interests.

Data availability

The novel immunopeptidomics data generated for this study is available in supplementary table 2 in the manuscript (provided in saghar_peptide_data.xlsx).

Funding information

Research reported in this publication was supported by the National Institute of Allergy and Infectious Diseases (NIAID), under award number 75N93019C00001.

References

1. Rocha, N. & Neefjes, J. MHC class II molecules on the move for successful antigen presentation. *Embo Journal* **27**, 1–5 (2008).
2. Reynisson, B. *et al.* Improved Prediction of MHC II Antigen Presentation through Integration and Motif Deconvolution of Mass Spectrometry MHC Eluted Ligand Data. *J Proteome Res* **19**, 2304–2315 (2020).
3. Arango, M. T. *et al.* HLA-DRB1 the notorious gene in the mosaic of autoimmunity. *Immunol Res* **65**, 82–98 (2017).
4. Erlich, H. *et al.* HLA DR-DQ haplotypes and genotypes and type 1 diabetes risk analysis of the type 1 diabetes genetics consortium families. *Diabetes* **57**, 1084–1092 (2008).
5. Hu, X. *et al.* Additive and interaction effects at three amino acid positions in HLA-DQ and HLA-DR molecules drive type 1 diabetes risk. *Nat Genet* **47**, 898–905 (2015).
6. Stepniak, D. *et al.* Large-scale characterization of natural ligands explains the unique gluten-binding properties of HLA-DQ2. *Journal of Immunology* **180**, 3268–3278 (2008).
7. Racle, J. *et al.* Machine learning predictions of MHC-II specificities reveal alternative binding mode of class II epitopes. *bioRxiv* 2022.06.26.497561 (2022) doi:10.1101/2022.06.26.497561.
8. Bergseng, E. *et al.* Different binding motifs of the celiac disease-associated HLA molecules DQ2.5, DQ2.2, and DQ7.5 revealed by relative quantitative proteomics of endogenous peptide repertoires. *Immunogenetics* **67**, 73–84 (2014).
9. Sidney, J. *et al.* Divergent motifs but overlapping binding repertoires of six HLA-DQ molecules frequently expressed in the worldwide human population. *Journal of Immunology* **185**, 4189–4198 (2010).
10. Vartdal, F. *et al.* The peptide binding motif of the disease associated HLA-DQ (α 1* 0501, β 1* 0201) molecule. *Eur J Immunol* **26**, 2764–2772 (1996).
11. Tollefsen, S. *et al.* Structural and functional studies of trans-encoded HLA-DQ2.3 (DQA1*03:01/DQB1*02:01) protein molecule. *Journal of Biological Chemistry* **287**, 13611–13619 (2012).
12. Kwok, W. W., Kovats, S., Thurtle, P. & Nepom, G. T. HLA-DQ allelic polymorphisms constrain patterns of class II heterodimer formation. *The Journal of Immunology* **150**, 2263–2272 (1993).
13. Creary, L. E. *et al.* High-resolution HLA allele and haplotype frequencies in several unrelated populations determined by next generation sequencing: 17th International HLA and Immunogenetics Workshop joint report. *Hum Immunol* **82**, 505–522 (2021).
14. Petersdorf, E. W. *et al.* HLA-DQ heterodimers in hematopoietic cell transplantation. *Blood* **139**, 3009–3017 (2022).
15. Lundin, K. E. *et al.* T lymphocyte recognition of a celiac disease-associated cis- or trans-encoded HLA-DQ alpha/beta-heterodimer. *The Journal of Immunology* **145**, 136–139 (1990).
16. Kwok, W. W. & Nepom, G. T. Structural and functional constraints on HLA class II dimers implicated in susceptibility to insulin dependent diabetes mellitus. *Baillieres Clin Endocrinol Metab* **5**, 375–393 (1991).
17. McFarland, B. J. & Beeson, C. Binding interactions between peptides and proteins of the class II Major Histocompatibility Complex. *Med Res Rev* **22**, 168–203 (2002).

855 18. Nielsen, M., Andreatta, M., Peters, B. & Buus, S. Immunoinformatics: Predicting Peptide–
856 MHC Binding. *Annu Rev Biomed Data Sci* **3**, 191–215 (2020).
857 19. Reynisson, B., Alvarez, B., Paul, S., Peters, B. & Nielsen, M. NetMHCpan-4.1 and
858 NetMHCIIpan-4.0: improved predictions of MHC antigen presentation by concurrent motif
859 deconvolution and integration of MS MHC eluted ligand data. *Nucleic Acids Res* **48**,
860 W449–W454 (2020).
861 20. Gfeller, D. & Bassani-Sternberg, M. Predicting antigen presentation-What could we learn
862 from a million peptides? *Front Immunol* **9**, 1716 (2018).
863 21. Nielsen, M., Lund, O., Buus, S. & Lundegaard, C. MHC Class II epitope predictive
864 algorithms. *Immunology* **130**, 319–328 (2010).
865 22. Bassani-Sternberg, M. *et al.* Direct identification of clinically relevant neoepitopes
866 presented on native human melanoma tissue by mass spectrometry. *Nat Commun* **7**,
867 13404 (2016).
868 23. Kaabinejadian, S. *et al.* Accurate MHC Motif Deconvolution of Immunopeptidomics Data
869 Reveals a Significant Contribution of DRB3, 4 and 5 to the Total DR Immunopeptidome.
870 *Front Immunol* **13**, 835454 (2022).
871 24. Alvarez, B., Barra, C., Nielsen, M. & Andreatta, M. Computational Tools for the
872 Identification and Interpretation of Sequence Motifs in Immunopeptidomes. *Proteomics*
873 **18**, 1700252 (2018).
874 25. Caron, E. *et al.* Analysis of major histocompatibility complex (MHC) immunopeptidomes
875 using mass spectrometry. *Molecular and Cellular Proteomics* **14**, 3105–3117 (2015).
876 26. Purcell, A. W., Ramarathinam, S. H. & Ternette, N. Mass spectrometry–based
877 identification of MHC-bound peptides for immunopeptidomics. *Nat Protoc* **14**, 1687–1707
878 (2019).
879 27. Barra, C. *et al.* Footprints of antigen processing boost MHC class II natural ligand
880 predictions. *Genome Med* **10**, (2018).
881 28. Paul, S. *et al.* Determination of a predictive cleavage motif for eluted major
882 histocompatibility complex class II ligands. *Front Immunol* **9**, 1795 (2018).
883 29. Racle, J. *et al.* Robust prediction of HLA class II epitopes by deep motif deconvolution of
884 immunopeptidomes. *Nat Biotechnol* **37**, 1283–1286 (2019).
885 30. Wang, P. *et al.* Peptide binding predictions for HLA DR, DP and DQ molecules. *BMC*
886 *Bioinformatics* **11**, 568 (2010).
887 31. Nielsen, M., Lundegaard, C. & Lund, O. Prediction of MHC class II binding affinity using
888 SMM-align, a novel stabilization matrix alignment method. *BMC Bioinformatics* **8**, 238
889 (2007).
890 32. Alvarez, B. *et al.* NNAlign_MA; MHC peptidome Deconvolution for Accurate MHC Binding
891 Motif Characterization and Improved T-cell Epitope Predictions. *Molecular and Cellular*
892 *Proteomics* **18**, 2459–2477 (2019).
893 33. Nielsen, M. & Andreatta, M. NetMHCpan-3.0; improved prediction of binding to MHC
894 class I molecules integrating information from multiple receptor and peptide length
895 datasets. *Genome Med* **8**, (2016).
896 34. Hoof, I. *et al.* NetMHCpan, a method for MHC class I binding prediction beyond humans.
897 *Immunogenetics* **61**, 1–13 (2009).

35. Karosiene, E. *et al.* NetMHCIIpan-3.0, a common pan-specific MHC class II prediction method including all three human MHC class II isotypes, HLA-DR, HLA-DP and HLA-DQ. *Immunogenetics* **65**, 711–724 (2013).
36. Gonzalez-Galarza, F. F., Christmas, S., Middleton, D. & Jones, A. R. Allele frequency net: A database and online repository for immune gene frequencies in worldwide populations. *Nucleic Acids Res* **39**, (2011).
37. Thomsen, M. C. F., Lundegaard, C., Buus, S., Lund, O. & Nielsen, M. MHCcluster, a method for functional clustering of MHC molecules. *Immunogenetics* **65**, 655–665 (2013).
38. Moore, R. M., Harrison, A. O., McAllister, S. M., Polson, S. W. & Eric Wommack, K. Iroki: Automatic customization and visualization of phylogenetic trees. *PeerJ* **8**, e8584 (2020).
39. Larkin, M. A. *et al.* Clustal W and Clustal X version 2.0. *Bioinformatics* **23**, 2947–2948 (2007).
40. Marcu, A. *et al.* HLA Ligand Atlas: A benign reference of HLA-presented peptides to improve T-cell-based cancer immunotherapy. *J Immunother Cancer* **9**, (2021).

Supplementary figures

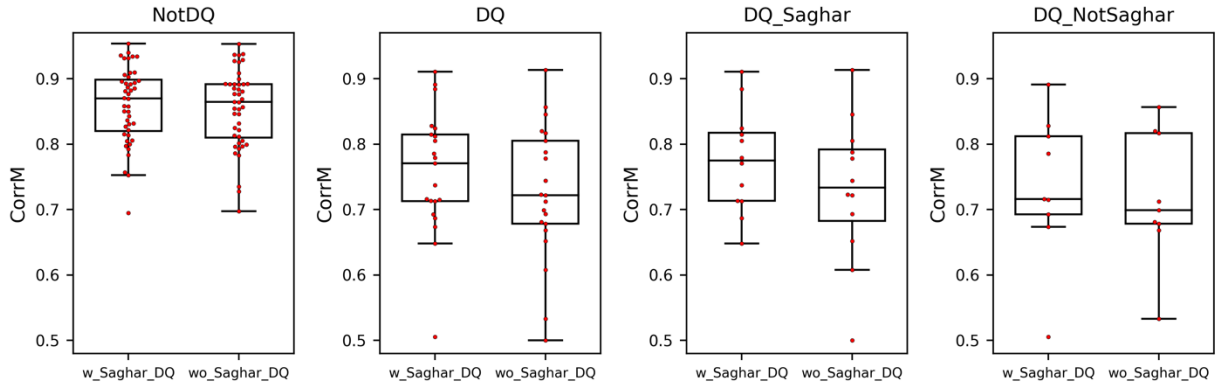

Supplementary figure 1: Mean consistency values for HLA molecule deconvolutions shared between multiple data sets for the two models. Each point reflects an HLA class II molecule, and values shown are the mean over the different data set comparisons. The different subgroups of HLA molecules are defined in the main text and the Figure 2 caption.

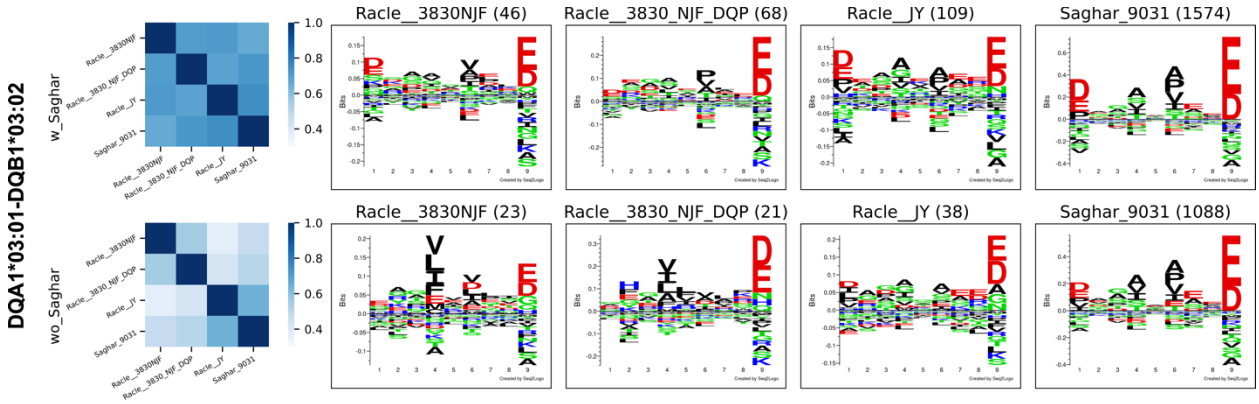

Supplementary figure 2: Consistency analysis for HLA-DQA1*03:01-DQB1*03:02. Here, only a subset of the cell lines used in the consistency analysis are included. Left panel: Correlation matrices showing the consistency values per cell line pair. Right panel: Sequence logos constructed from the peptide sets used in the consistency correlation analysis, with a minimum threshold of 20 peptides required for a given logo. The rows correspond to the methods including (w_Saghar) and not including (wo_Saghar) the novel data. The peptide count for each logo is shown in parenthesis in the logo title.

Supplementary figure 3: Identified binding motifs for the 14 DQ molecules from the novel data in the two methods. Left panel: Motif deconvolution of the novel datasets in the models trained with (wSag) and without (woSag) the novel data (the two rows with 4 logos correspond to the two HLA-DQ molecules shared between two cell lines). Right panel: Motifs predicted for the HLA-DQ molecules by the two models. Predicted motifs are generated from the top 1% of 100,000 random natural 13-17 mer peptides.

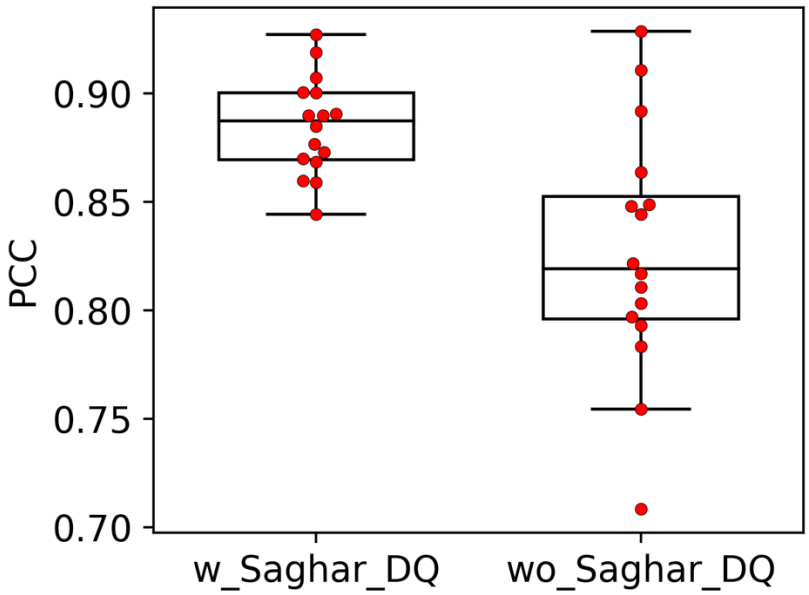

Supplementary figure 4: Correlations between deconvoluted and predicted sequence logos in the methods with (w_Saghar) and without (wo_Saghar) the novel data. For each cell line in the novel data, the PCC value between the DQ motif deconvolution PSSM and predicted PSSM for the corresponding molecule was calculated for each of the methods with and without the novel data.

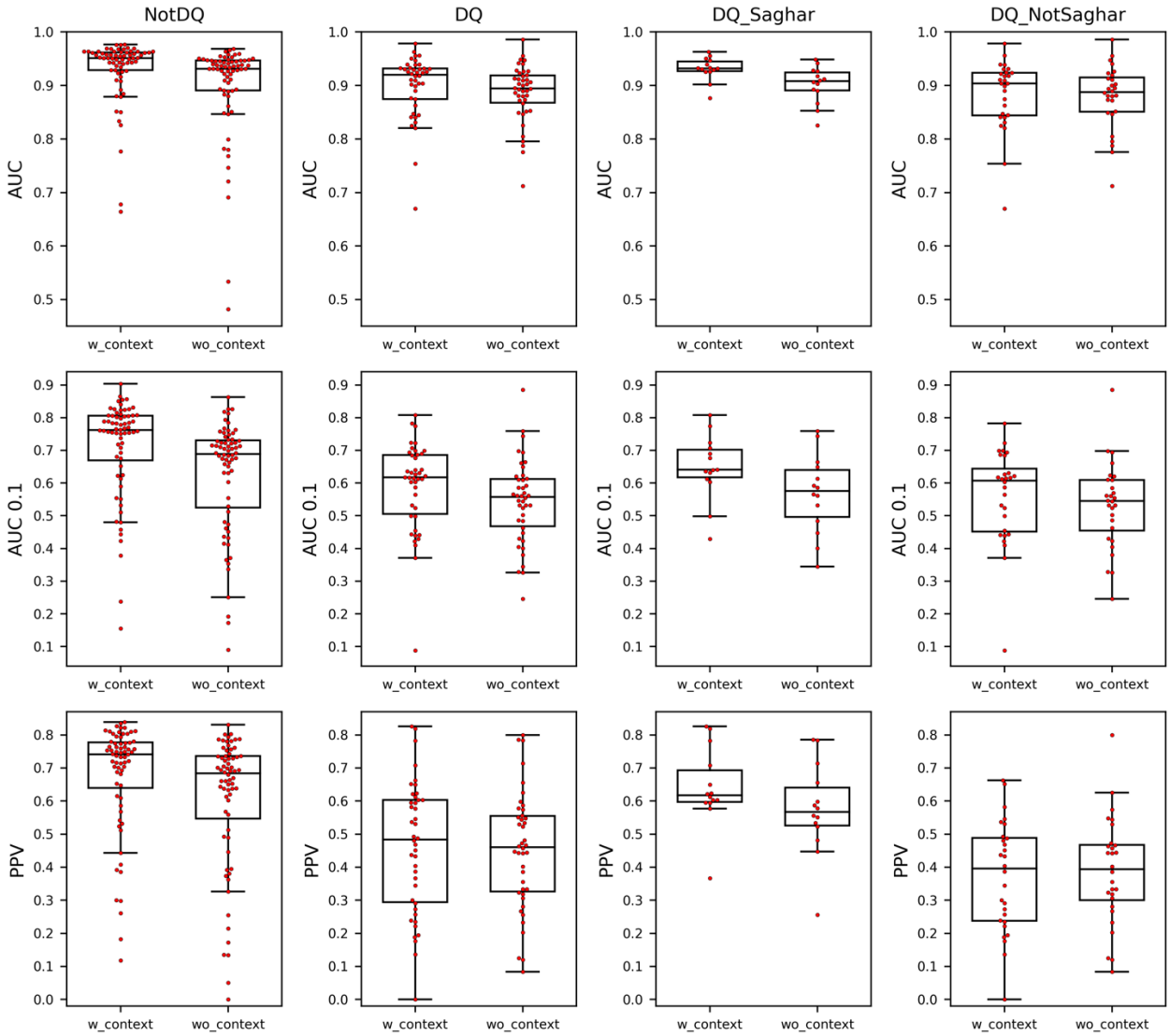

Supplementary figure 5: **Performance comparison of models trained with the novel DQ data, with (w_context) and without (wo_context) context encoding**. The different subgroups of HLA molecules are defined in the main text and the Figure 2 caption.

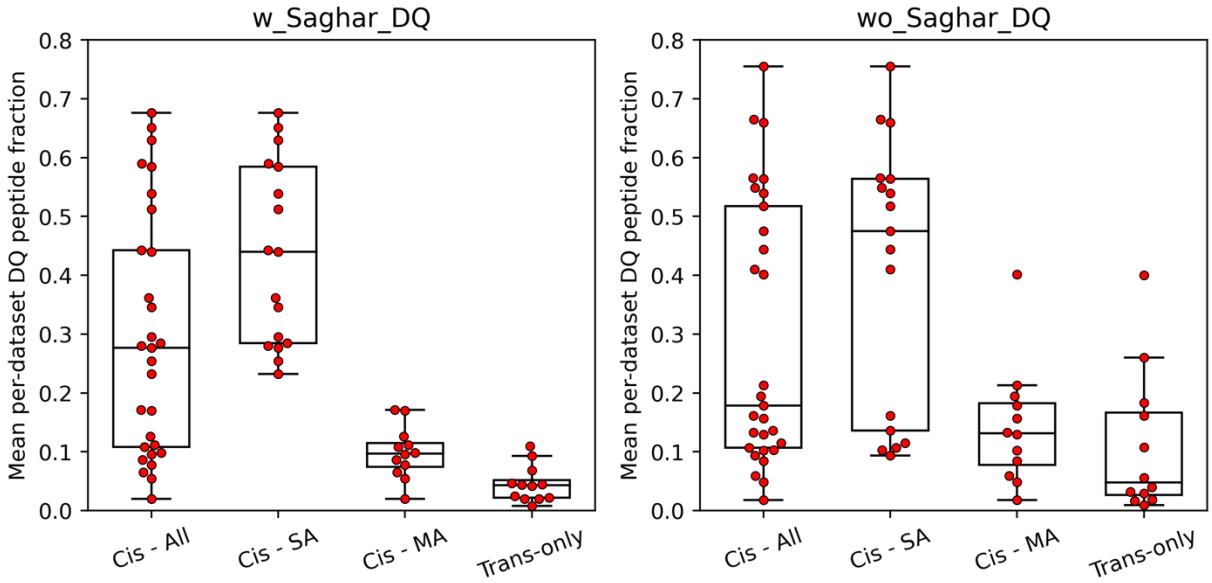

Supplementary figure 6: Peptide-count contribution of cis and trans-only molecules in the methods with (w_Saghar_DQ) and without (wo_Saghar_DQ) the novel data, taking into account pseudo-sequence overlap. Each point shows the mean per-dataset peptide fraction for a given DQ molecule. The cis molecules are shown in three categories, namely all cis molecules (Cis - All), cis molecules found in the DQ-SA training data or with the same pseudosequence as a DQ-SA molecule (Cis - SA), and cis molecules only found in the DQ-MA training data and with no pseudosequence overlap to cis-SA molecules (Cis - MA). Here, a significant difference was found between cis-MA and trans-only in the model with the novel data (p=0.002, two-sample t-test).

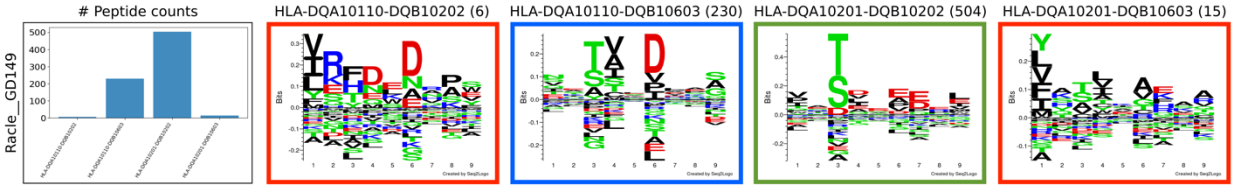

Supplementary figure 7: DQ motif deconvolution of the Racle__GD149 dataset. The logo frame colors indicate three types of DQ molecules, namely cis-molecules present in the DQ-SA training data (green), cis molecules present in the DQ-MA training data (blue), and trans-only molecules (red).

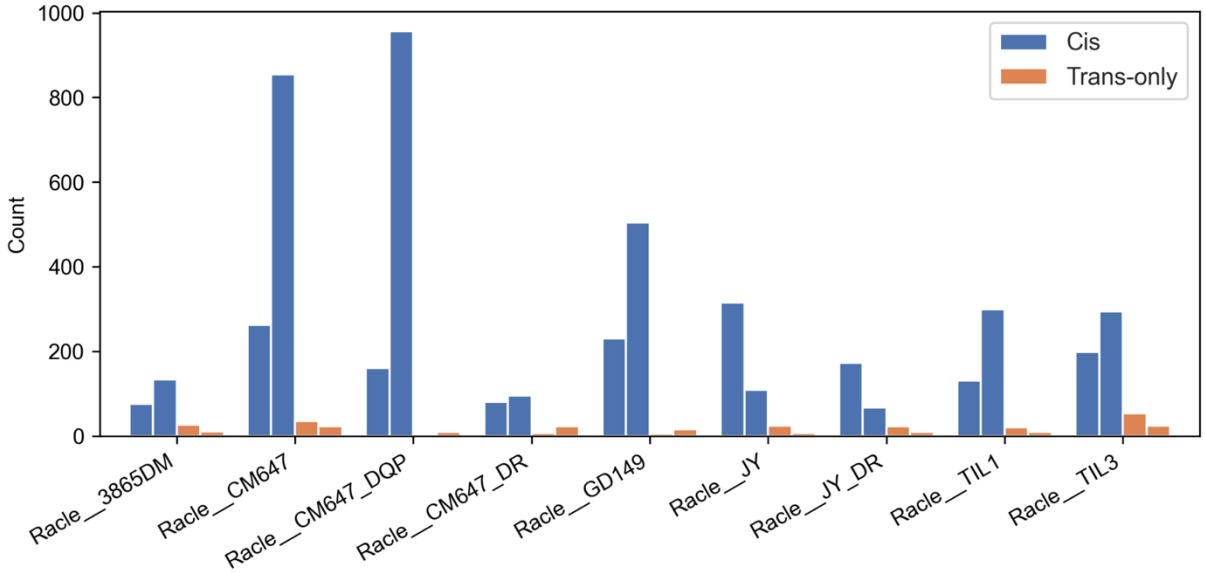

Supplementary figure 8: DQ ligand count distributions in DQ-heterozygous cell lines with both cis and trans-only molecules. Only cell lines with at least 100 DQ-annotated peptides excluding trash are included. The counts are shown for the individual molecules, colored by category (cis: blue and trans-only: orange). If we assume that the relative expression from each chromosome is linked to the observed peptide counts for the cis variants, then the trans-only variants (if they were functional) should in principle have peptide counts corresponding to at least the cis variant with the lowest count. However, this is not what we observe, as the cis variant with the lowest count always has a much larger peptide count than both trans-only variants.

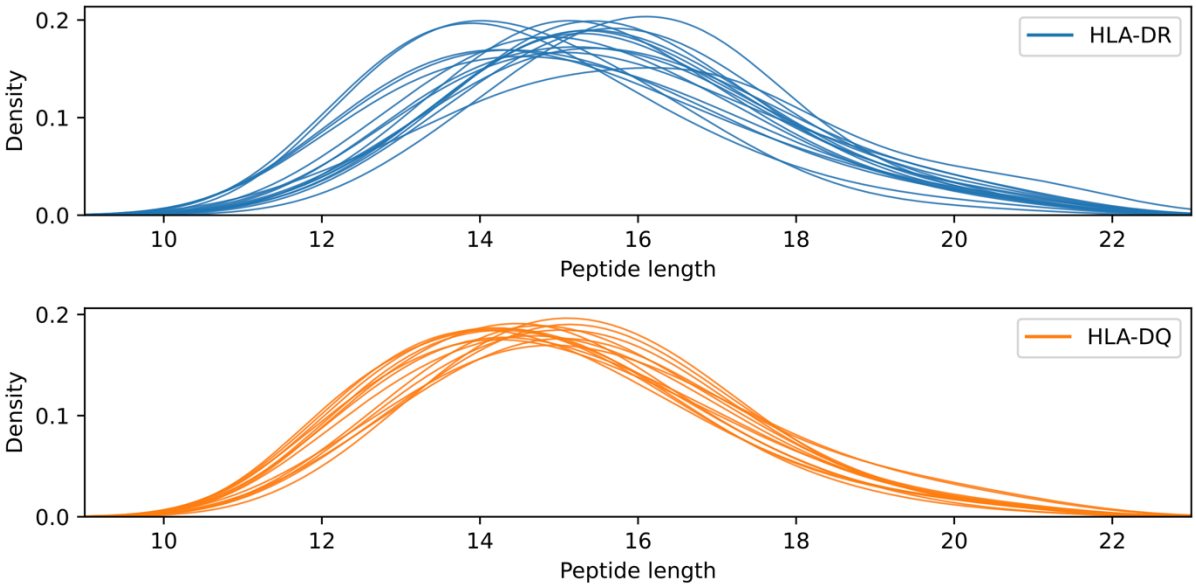

Supplementary figure 9: Kernel density plots of length distributions of peptides extracted from the cell lines used in the novel data. Each curve corresponds to the peptide length distribution for an HLA-DR (top) or HLA-DQ (bottom) molecule. The DR distributions are based on the immunopeptidomics data from supplementary table 4 in Kaabinejadian et al. 2022, which were run through the motif deconvolution method developed in this manuscript.

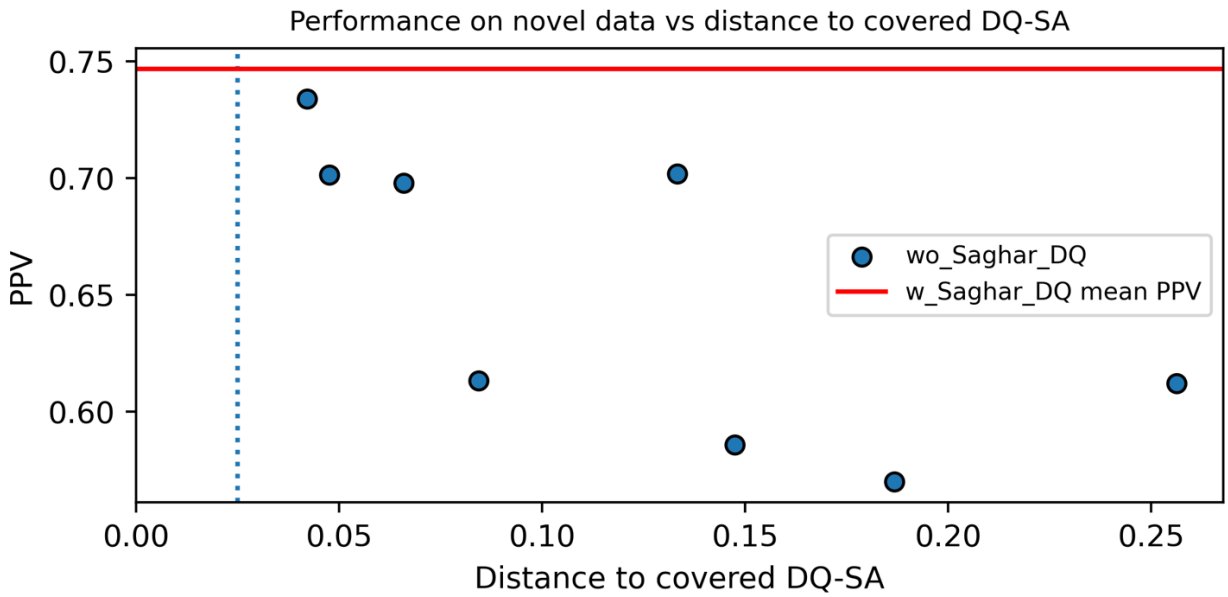

Supplementary figure 10: Performance vs distance analysis for the model trained without the novel data (wo_Saghar_DQ). Each point shows the PPV performance evaluated on the novel data for a DQ molecule not present in the DQ-SA training data of the wo_Saghar_DQ method, as a function of the distance to the training data DQ-SA molecules. The red line shows the mean performance of the model trained with the novel data (w_Saghar_DQ) on the same set of DQ molecules, evaluated on the novel data.

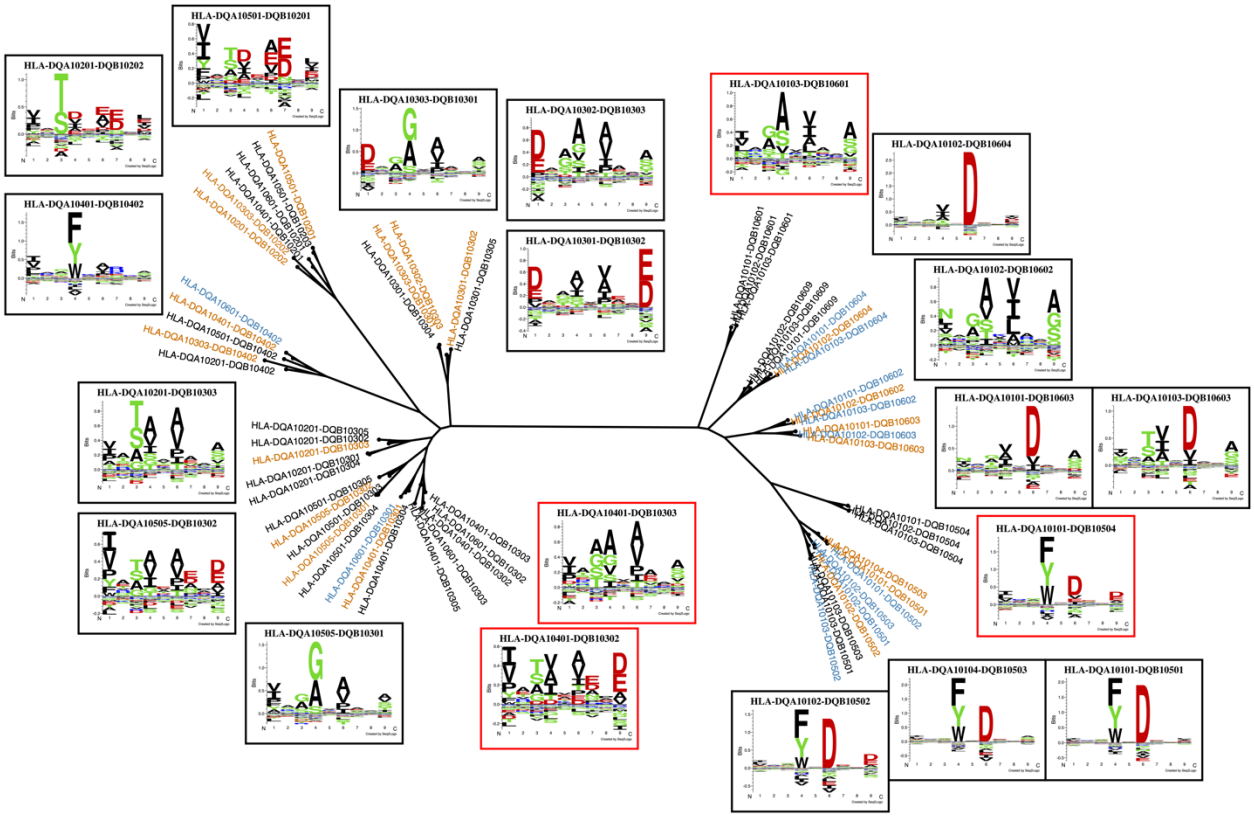

Supplementary figure 11: Sequence-based clustering of DQ molecules. The tree is based on 61 DQ molecules including the 14 molecules described by the novel data. Orange molecules are covered by the method including the novel data with at least 100 peptides, and blue molecules are within a distance 0.025 of an orange molecule. Black molecules are non-covered (i.e. have peptide count less than 100 and have distance greater than 0.025 to an orange molecule). Logos in black frames correspond to orange molecules. Logos in red frames correspond to molecules from branches with clusters of non-covered (black) molecules. The phylogenetic tree was constructed from the DQ pseudo-sequences using ClustalW. Logos were constructed from the top 1% of 100,000 random 13-17 mer peptides.

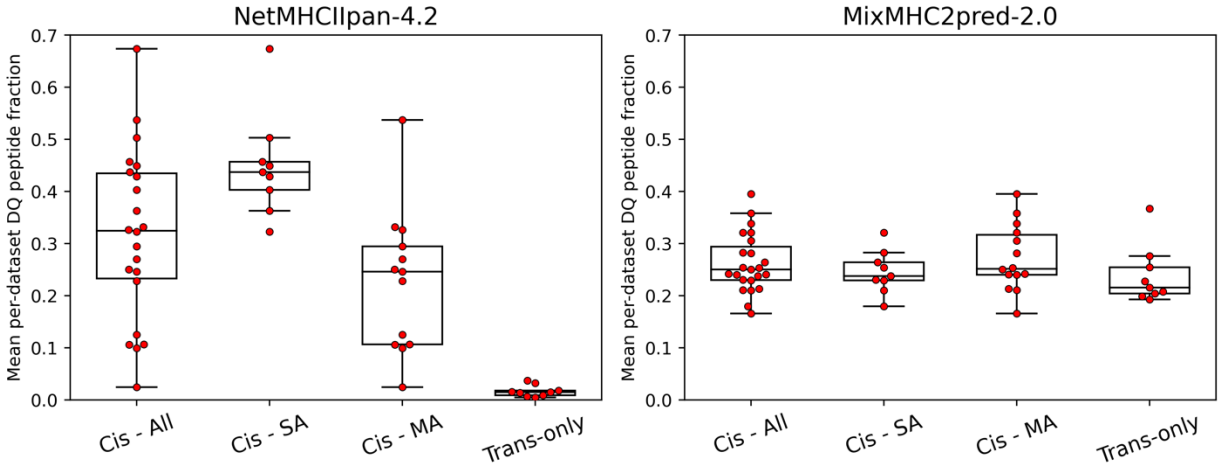

Supplementary figure 12A: Peptide-count contribution of cis and trans-only molecules predicted by NetMHCIIpan-4.2 and MixMHC2pred-2.0 on DQ-heteryzygous data from Marcu et al. 2021. Each point shows the mean per-dataset peptide fraction for a given DQ molecule. The cis molecules are shown in three categories, namely all cis molecules (Cis - All), cis molecules found in the DQ-SA training data (Cis - SA), and cis molecules only found in the DQ-MA training data (Cis - MA).

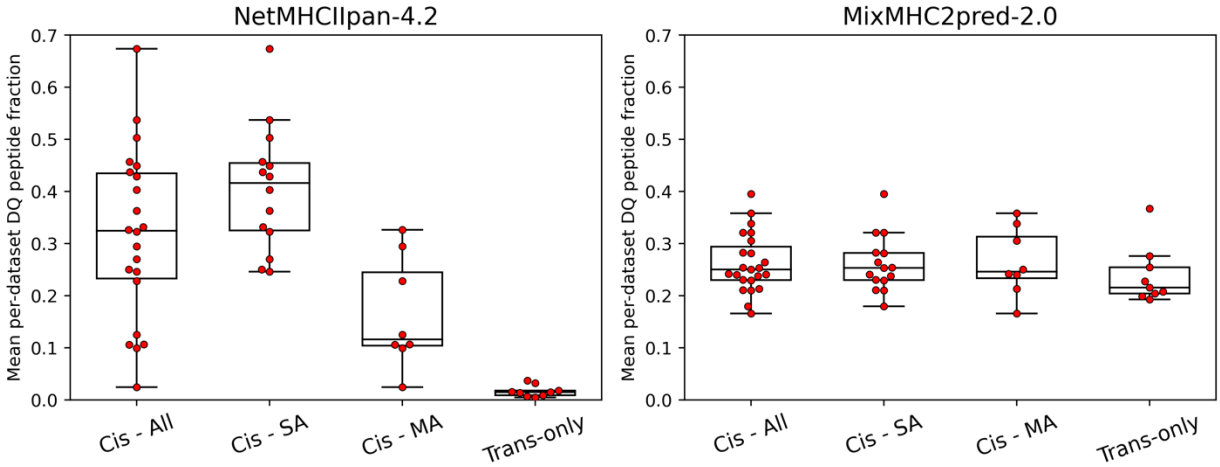

Supplementary figure 12B: Peptide-count contribution of cis and trans-only molecules predicted by NetMHCIIpan-4.2 and MixMHC2pred-2.0 on DQ-heteryzygous data from Marcu et al. 2021, taking into account pseudo-sequence overlap. Each point shows the mean per-dataset peptide fraction for a given DQ molecule. The cis molecules are shown in three categories, namely all cis molecules (Cis - All), cis molecules found in the DQ-SA training data or with the same pseudosequence as a DQ-SA molecule (Cis - SA), and cis molecules only found in the DQ-MA training data and with no pseudosequence overlap to cis-SA molecules (Cis - MA). Here, a significant difference was found between cis-MA and trans-only in NetMHCIIpan-4.2 (p=0.001, two-sample t-test).

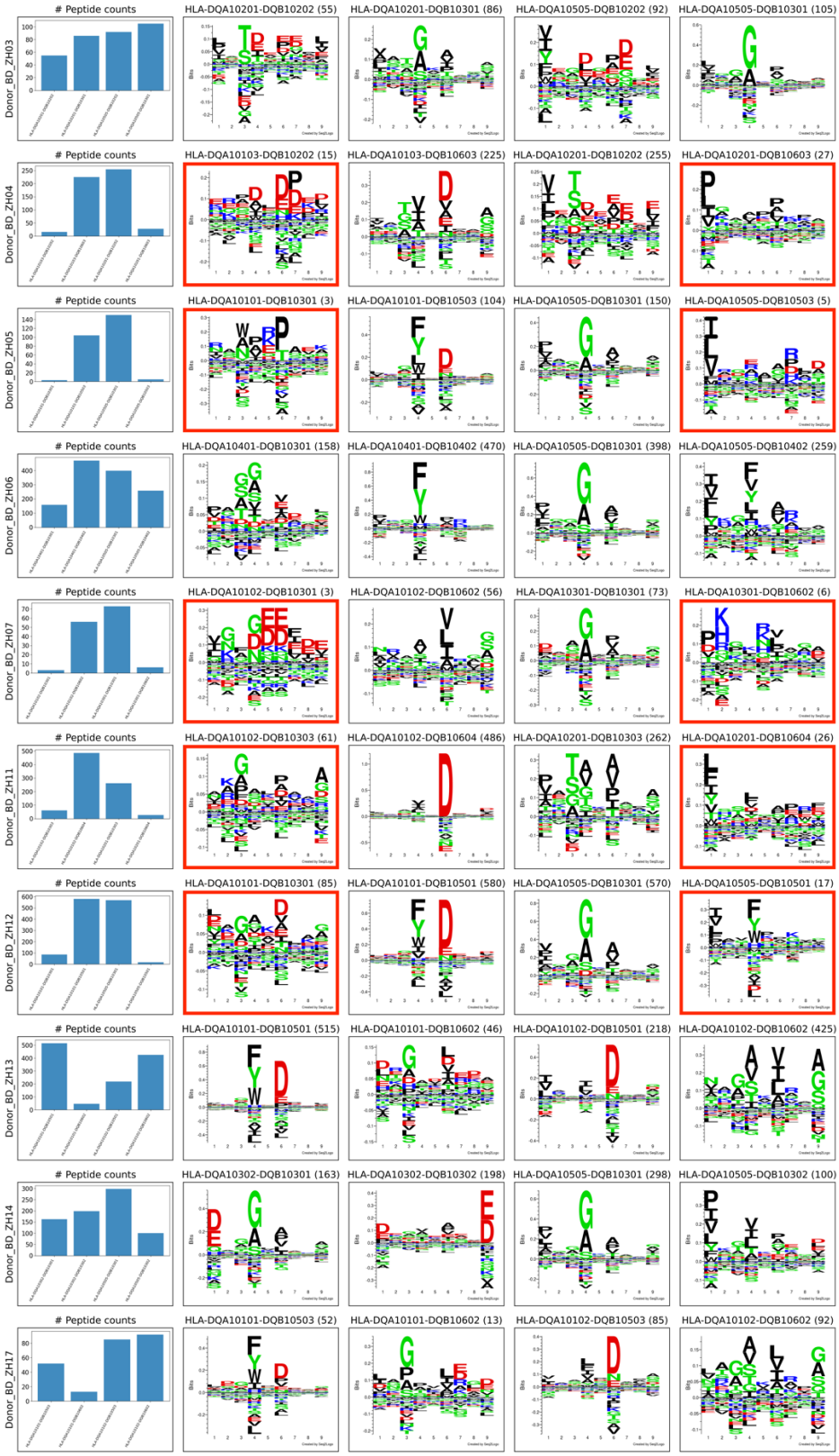

Supplementary figure 12C: DQ motif deconvolution for DQ-heterozygous datasets in the benchmark data from Marcu et al. 2021. Each row corresponds to a donor sample. Only peptides with percentile rank less than 5 were included in the logo plots. Trans-only molecules are highlighted in red frames.

1029 # Supplementary tables

1030

1031 **Supplementary table 1: Overview of HLA types per EL dataset used to train our method.** The novel data
1032 generated for this study are highlighted in bold. For two of the datasets from Abelin et al. 2019
1033 (Abelin__HLA_DR_SILAC_Donor2_DC_UV_16hr and Abelin__HLA_DR_SILAC_Donor2_DC_UV_24hr), the original
1034 HLA typing was listed to have only two DQ molecules. However, we believe this to be an erroneous HLA typing, as
1035 the cell lines should express four different DQ molecules. As such, the HLA typing for these datasets was extended to
1036 include all four DQ heterodimers.

Sample	HLA type
Saghar_721	**DRB1*01:01,DQA1*01:01-DQB1*05:01,DPA1*01:03-DPB1*02:01**
Saghar_9004	**DRB1*01:01,DQA1*01:01-DQB1*05:01,DPA1*01:03-DPB1*04:01**
Saghar_9013	**DRB1*15:01,DRB5*01:01,DQA1*01:02-DQB1*06:02,DPA1*01:03-DPB1*04:02**
Saghar_9023	**DRB1*03:01,DRB3*01:01,DQA1*05:01-DQB1*02:01,DPA1*02:01-DPB1*01:01**
Saghar_9031	**DRB1*04:01,DRB4*01:03,DQA1*03:01-DQB1*03:02,DPA1*01:03-DPB1*04:01**
Saghar_9043	**DRB1*11:01,DRB3*02:02,DQA1*05:05-DQB1*03:01,DPA1*02:01-DPB1*10:01**
Saghar_9052	**DRB1*07:01,DRB4*01:03N,DQA1*02:01-DQB1*03:03,DPA1*01:03-DPB1*04:01**
Saghar_9060	**DRB1*13:01,DRB3*02:02,DQA1*01:03-DQB1*06:03,DPA1*02:02-DPB1*19:01**
Saghar_9061	**DRB1*14:01,DRB3*02:02,DQA1*01:04-DQB1*05:03,DPA1*01:03-DPB1*04:01**
Saghar_9063	**DRB1*13:02,DRB3*03:01,DQA1*01:02-DQB1*06:04,DPA1*01:03-DPB1*16:01**
Saghar_9072	**DRB1*08:02,DQA1*04:01-DQB1*04:02,DPA1*01:03-DPB1*04:02**
Saghar_9075	**DRB1*09:01,DRB4*01:03,DQA1*03:02-DQB1*03:03,DPA1*01:03-DPB1*04:01**
Saghar_9084	**DRB1*16:01,DRB5*02:02,DQA1*01:02-DQB1*05:02,DPA1*01:03-DPB1*04:01**
Saghar_9090	**DRB1*04:01,DRB4*01:03,DQA1*03:03-DQB1*03:01,DPA1*01:03-DPB1*04:01,DPA1*01:03-DPB1*14:01,DPA1*02:01-DPB1*04:01,DPA1*02:01-DPB1*14:01**
Saghar_9093	**DRB1*07:01,DRB4*01:03,DQA1*02:01-DQB1*02:02,DPA1*01:03-DPB1*02:01,DPA1*01:03-DPB1*04:01**
Saghar_9100	**DRB1*08:02,DQA1*04:01-DQB1*04:02,DPA1*01:03-DPB1*03:01,DPA1*01:03-DPB1*04:02**
Abelin__MAPTAC_DRB1_0403	DRB1*04:03
Abelin__MAPTAC_DRB1_0803	DRB1*08:03
Abelin__MAPTAC_DRB5_0101	DRB5*01:01
Abelin__MAPTAC_DRB3_0202	DRB3*02:02
Abelin__MAPTAC_DPB1_0601_DPA1_0103_dmPos	DPA1*01:03-DPB1*06:01
Abelin__MAPTAC_DQB1_0604_DQA1_0102_dmPos	DQA1*01:02-DQB1*06:04
Abelin__MAPTAC_HLA_DPB10201_DPA10103	DPA1*01:03-DPB1*02:01
Abelin__MAPTAC_HLA_DQB10602_DQA10102	DQA1*01:02-DQB1*06:02
Abelin__MAPTAC_DRB1_0101	DRB1*01:01
Abelin__MAPTAC_DRB1_0102	DRB1*01:02
Abelin__MAPTAC_DRB1_0301	DRB1*03:01
Abelin__MAPTAC_DRB1_0302	DRB1*03:02
Abelin__MAPTAC_DRB1_0401	DRB1*04:01
Abelin__MAPTAC_DRB1_0402	DRB1*04:02

Abelin__MAPTAC_DRB1_0404	DRB1*04:04
Abelin__MAPTAC_DRB1_0405	DRB1*04:05
Abelin__MAPTAC_DRB1_0407	DRB1*04:07
Abelin__MAPTAC_DRB1_0701	DRB1*07:01
Abelin__MAPTAC_DRB1_0801	DRB1*08:01
Abelin__MAPTAC_DRB1_0802	DRB1*08:02
Abelin__MAPTAC_DRB1_0804	DRB1*08:04
Abelin__MAPTAC_DRB1_0901	DRB1*09:01
Abelin__MAPTAC_DRB1_1001	DRB1*10:01
Abelin__MAPTAC_DRB1_1101	DRB1*11:01
Abelin__MAPTAC_DRB1_1102	DRB1*11:02
Abelin__MAPTAC_DRB1_1104	DRB1*11:04
Abelin__MAPTAC_DRB1_1202	DRB1*12:02
Abelin__MAPTAC_DRB1_1301	DRB1*13:01
Abelin__MAPTAC_DRB1_1302	DRB1*13:02
Abelin__MAPTAC_DRB1_1303	DRB1*13:03
Abelin__MAPTAC_DRB1_1401	DRB1*14:01
Abelin__MAPTAC_DRB1_1501	DRB1*15:01
Abelin__MAPTAC_DRB1_1502	DRB1*15:02
Abelin__MAPTAC_DRB1_1503	DRB1*15:03
Abelin__MAPTAC_DRB1_1601	DRB1*16:01
Abelin__MAPTAC_DRB3_0301	DRB3*03:01
Abelin__MAPTAC_DRB4_0103	DRB4*01:03
Abelin__MAPTAC_DRB1_1201	DRB1*12:01
Abelin__MAPTAC_DRB3_0101	DRB3*01:01
Abelin__HLA_DR_A375	DRB1*07:01,DRB4*01:01,DRB1*04:05
Abelin__HLA_DR_Lung	DRB1*01:01,DRB1*03:01,DRB3*01:01,DPA1*01:03-DPB1*02:01,DPA1*02:01-DPB1*02:01,DPA1*01:03-DPB1*10:01,DPA1*02:01-DPB1*10:01,DQA1*01:01-DQB1*02:01,DQA1*01:01-DQB1*05:01,DQA1*05:01-DQB1*02:01,DQA1*05:01-DQB1*05:01
Abelin__HLA_DR_PBMC_HDSC	DRB1*03:01,DRB1*11:01,DRB3*01:01,DRB3*02:02
Abelin__HLA_DR_PBMC_RG1095	DRB1*03:01,DRB1*11:01,DRB3*01:01,DRB3*02:02
Abelin__HLA_DR_PBMC_RG1104	DRB1*01:01,DRB1*11:01,DRB3*02:02
Abelin__HLA_DR_PBMC_RG1248	DRB1*03:01,DRB3*01:01
Abelin__HLA_DR_SILAC_Donor1_10minLysate	DRB1*07:01,DRB4*01:01
Abelin__HLA_DR_SILAC_Donor1_5hrLysate	DRB1*07:01,DRB4*01:01
Abelin__HLA_DR_SILAC_Donor1_DConly	DRB1*07:01,DRB4*01:01
Abelin__HLA_DR_SILAC_Donor1_UVovernight	DRB1*07:01,DRB4*01:01
Abelin__HLA_DR_SILAC_Donor2_DC_UV_16hr	DRB1*04:01,DRB4*01:03,DRB1*15:03,DRB5*01:01,DQA1*03:01-DQB1*03:02,DQA1*01:02-DQB1*06:02,DQA1*01:02-DQB1*03:02,DQA1*03:01-DQB1*06:02,DPA1*01:03-DPB1*02:01,DPA1*01:03-DPB1*04:01

Abelin__HLA_DR_SILAC_Donor2_DC_UV_24hr	DRB1*04:01,DRB4*01:03,DRB1*15:03,DRB5*01:01,DQA1*03:01-DQB1*03:02,DQA1*01:02-DQB1*06:02,DQA1*01:02-DQB1*03:02,DQA1*03:01-DQB1*06:02,DPA1*01:03-DPB1*02:01,DPA1*01:03-DPB1*04:01
Abelin__HLA_DR_Spleen	DRB1*01:01,DRB1*03:01,DRB3*01:01,DPA1*01:03-DPB1*02:01,DPA1*02:01-DPB1*02:01,DPA1*01:03-DPB1*10:01,DPA1*02:01-DPB1*10:01,DQA1*01:01-DQB1*02:01,DQA1*01:01-DQB1*05:01,DQA1*05:01-DQB1*02:01,DQA1*05:01-DQB1*05:01
Benito__T2_DR3	DRB1*03:01,DRB3*01:01
Bergseng__9037_SWEIG	DRB1*11:01,DRB3*02:02,DQA1*05:05-DQB1*03:01,DPA1*01:03-DPB1*04:02
Bergseng__9047_PLH	DRB1*07:01,DRB4*01:01,DQA1*02:01-DQB1*02:02,DPA1*01:03-DPB1*15:01
Bergseng__9050_MOU	DRB1*07:01,DRB4*01:01,DQA1*02:01-DQB1*02:02,DPA1*01:03-DPB1*02:01
Bergseng__9051_PITOUT	DRB1*07:01,DRB4*01:01,DQA1*02:01-DQB1*02:02,DPA1*01:03-DPB1*04:01
Bergseng__9064_AMALA	DRB1*14:02,DRB3*01:01,DQA1*05:01-DQB1*03:01,DQA1*05:03-DQB1*03:01,DPA1*01:03-DPB1*04:02,DPA1*01:03-DPB1*94:01
Bergseng__9087_STEINLIN	DRB1*03:01,DRB3*01:01,DQA1*05:01-DQB1*02:01,DPA1*01:03-DPB1*03:01,DPA1*01:03-DPB1*04:01
Bergseng__9088_PF04015	DRB1*03:01,DRB3*01:01,DQA1*05:01-DQB1*02:01,DPA1*01:03-DPB1*01:01,DPA1*02:01-DPB1*04:01,DPA1*01:03-DPB1*04:01,DPA1*02:01-DPB1*01:01
Bergseng__9089_BOB	DRB1*11:04,DRB3*02:02,DQA1*05:05-DQB1*03:01,DPA1*01:03-DPB1*04:02
Clement__DRB1_0101	DRB1*01:01
Heyder__Bcell	DRB1*04:01,DRB4*01:01
Heyder__PAT1	DRB1*04:01,DRB1*07:01,DRB4*01:01
Heyder__PAT7	DRB1*03:01,DRB1*15:01,DRB3*01:01,DRB5*01:01
Karuna__H_2_IAb	H-2-IAb
Khoda__Jeko	DRB1*04:03,DRB1*07:01,DRB4*01:01
Khoda__L128	DRB1*07:01,DRB1*11:01,DRB4*01:01,DRB3*02:02
Khoda__MCL001	DRB1*04:02,DRB1*07:01,DRB4*01:01
Khoda__MCL005	DRB1*04:01,DRB1*11:04,DRB4*01:01,DRB3*02:02
Khoda__MCL008	DRB1*04:01,DRB1*13:01,DRB4*01:01,DRB3*01:01
Khoda__MCL022	DRB1*01:03,DRB1*04:01,DRB4*01:01
Khoda__MCL030	DRB1*07:01,DRB1*13:03,DRB4*01:01
Khoda__MCL034	DRB1*03:01,DRB1*04:01,DRB3*01:01,DRB4*01:01
Khoda__MCL037	DRB1*11:01,DRB1*14:54,DRB3*02:02
Khoda__MCL041	DRB1*04:01,DRB1*13:01,DRB4*01:01,DRB3*01:01
Khoda__MCL043	DRB1*07:01,DRB1*11:01,DRB4*01:01,DRB3*02:02
Khoda__MCL049	DRB1*01:01,DRB1*07:01,DRB4*01:01
Khoda__MCL052	DRB1*01:01,DRB1*13:01,DRB3*01:01
Khoda__MCLX001	DRB1*01:01,DRB1*07:01,DRB4*01:01
Khoda__MCLX002	DRB1*07:01,DRB1*13:01,DRB4*01:01,DRB3*01:01
Nanaware__WT_1	DRB1*01:01,DQA1*01:01-DQB1*05:01,DPA1*01:03-DPB1*04:01
Nanaware__WT_2	DRB1*01:01,DQA1*01:01-DQB1*05:01,DPA1*01:03-DPB1*04:01
Nanaware__WT_H2	H-2-IAb
Nelde__UPN1	DRB1*08:03,DRB1*13:01,DRB3*01:01

Nelde__UPN2	DRB1*08:01,DRB1*13:02,DRB3*03:01
Nelde__UPN3	DRB1*07:01,DRB1*08:01,DRB4*01:01
Ooi__DR15_human	DRB1*15:01,DRB5*01:01
Ooi__DR15_mouse	DRB1*15:01,DRB5*01:01
Ooi__DR1_human	DRB1*01:01
Ooi__DR1_mouse	DRB1*01:01
Racle__3808_HMC	DRB1*03:01,DRB1*07:01,DRB3*01:01,DRB4*01:01,DQA1*02:01-DQB1*02:01,DQA1*02:01-DQB1*02:02,DQA1*05:01-DQB1*02:01,DQA1*05:01-DQB1*02:02,DPA1*01:03-DPB1*03:01,DPA1*01:03-DPB1*11:01,DPA1*02:01-DPB1*03:01,DPA1*02:01-DPB1*11:01
Racle__3808_HMC_DQP	DRB1*03:01,DRB1*07:01,DRB3*01:01,DRB4*01:01,DQA1*02:01-DQB1*02:01,DQA1*02:01-DQB1*02:02,DQA1*05:01-DQB1*02:01,DQA1*05:01-DQB1*02:02,DPA1*01:03-DPB1*03:01,DPA1*01:03-DPB1*11:01,DPA1*02:01-DPB1*03:01,DPA1*02:01-DPB1*11:01
Racle__3808_HMC_DR	DRB1*03:01,DRB1*07:01,DRB3*01:01,DRB4*01:01,DQA1*02:01-DQB1*02:01,DQA1*02:01-DQB1*02:02,DQA1*05:01-DQB1*02:01,DQA1*05:01-DQB1*02:02,DPA1*01:03-DPB1*03:01,DPA1*01:03-DPB1*11:01,DPA1*02:01-DPB1*03:01,DPA1*02:01-DPB1*11:01
Racle__3830NJF	DRB1*04:04,DRB1*11:01,DRB3*02:02,DRB4*01:03,DQA1*03:01-DQB1*03:01,DQA1*03:01-DQB1*03:02,DQA1*05:05-DQB1*03:01,DQA1*05:05-DQB1*03:02,DPA1*01:03-DPB1*02:01,DPA1*01:03-DPB1*06:01
Racle__3830_NJF_DQP	DRB1*04:04,DRB1*11:01,DRB3*02:02,DRB4*01:03,DQA1*03:01-DQB1*03:01,DQA1*03:01-DQB1*03:02,DQA1*05:05-DQB1*03:01,DQA1*05:05-DQB1*03:02,DPA1*01:03-DPB1*02:01,DPA1*01:03-DPB1*06:01
Racle__3830_NJF_DR	DRB1*04:04,DRB1*11:01,DRB3*02:02,DRB4*01:03,DQA1*03:01-DQB1*03:01,DQA1*03:01-DQB1*03:02,DQA1*05:05-DQB1*03:01,DQA1*05:05-DQB1*03:02,DPA1*01:03-DPB1*02:01,DPA1*01:03-DPB1*06:01
Racle__3849BR	DRB1*11:04,DRB3*02:02,DQA1*05:05-DQB1*03:01,DPA1*01:03-DPB1*02:01,DPA1*01:03-DPB1*04:01
Racle__3865DM	DRB1*01:01,DRB1*07:01,DRB4*01:03,DQA1*01:01-DQB1*03:03,DQA1*01:01-DQB1*05:01,DQA1*02:01-DQB1*03:03,DQA1*02:01-DQB1*05:01,DPA1*01:03-DPB1*04:01,DPA1*01:03-DPB1*20:01
Racle__3869_GA	DRB1*01:03,DRB1*04:04,DRB4*01:03,DQA1*03:01-DQB1*03:01,DQA1*03:01-DQB1*03:02,DQA1*05:05-DQB1*03:01,DQA1*05:05-DQB1*03:02,DPA1*01:03-DPB1*04:01,DPA1*01:03-DPB1*12:60
Racle__3869_GA_DQP	DRB1*01:03,DRB1*04:04,DRB4*01:03,DQA1*03:01-DQB1*03:01,DQA1*03:01-DQB1*03:02,DQA1*05:05-DQB1*03:01,DQA1*05:05-DQB1*03:02,DPA1*01:03-DPB1*04:01,DPA1*01:03-DPB1*12:60
Racle__3869_GA_DR	DRB1*01:03,DRB1*04:04,DRB4*01:03,DQA1*03:01-DQB1*03:01,DQA1*03:01-DQB1*03:02,DQA1*05:05-DQB1*03:01,DQA1*05:05-DQB1*03:02,DPA1*01:03-DPB1*04:01,DPA1*01:03-DPB1*12:60
Racle__3911_ME	DRB1*11:01,DRB3*02:02,DQA1*05:05-DQB1*03:01,DPA1*01:03-DPB1*04:01
Racle__3912BAM	DRB1*03:01,DRB1*04:01,DRB3*01:01,DRB4*01:03,DQA1*03:01-DQB1*02:01,DQA1*03:01-DQB1*03:02,DQA1*05:01-DQB1*02:01,DQA1*05:01-DQB1*03:02,DPA1*01:03-DPB1*04:01
Racle__3912_BAM_DQP	DRB1*03:01,DRB1*04:01,DRB3*01:01,DRB4*01:03,DQA1*03:01-DQB1*02:01,DQA1*03:01-DQB1*03:02,DQA1*05:01-DQB1*02:01,DQA1*05:01-DQB1*03:02,DPA1*01:03-DPB1*04:01
Racle__3912_BAM_DR	DRB1*03:01,DRB1*04:01,DRB3*01:01,DRB4*01:03,DQA1*03:01-DQB1*02:01,DQA1*03:01-DQB1*03:02,DQA1*05:01-DQB1*02:01,DQA1*05:01-DQB1*03:02,DPA1*01:03-DPB1*04:01
Racle__3947_GA	DRB1*01:01,DRB1*13:01,DRB3*01:01,DQA1*01:01-DQB1*05:01,DQA1*01:01-DQB1*06:03,DQA1*01:03-DQB1*05:01,DQA1*01:03-DQB1*06:03,DPA1*01:03-DPB1*02:01,DPA1*01:03-DPB1*04:02
Racle__3947_GA_DQP	DRB1*01:01,DRB1*13:01,DRB3*01:01,DQA1*01:01-DQB1*05:01,DQA1*01:01-DQB1*06:03,DQA1*01:03-DQB1*05:01,DQA1*01:03-DQB1*06:03,DPA1*01:03-DPB1*02:01,DPA1*01:03-DPB1*04:02
Racle__3947_GA_DR	DRB1*01:01,DRB1*13:01,DRB3*01:01,DQA1*01:01-DQB1*05:01,DQA1*01:01-DQB1*06:03,DQA1*01:03-DQB1*05:01,DQA1*01:03-DQB1*06:03,DPA1*01:03-DPB1*02:01,DPA1*01:03-DPB1*04:02
Racle__3971_ORA	DRB1*13:03,DRB1*07:01,DRB3*01:01,DRB4*01:01,DQA1*02:01-DQB1*02:02,DQA1*02:01-DQB1*03:01,DQA1*05:05-DQB1*02:02,DQA1*05:05-DQB1*03:01,DPA1*01:03-DPB1*04:01,DPA1*02:02-DPB1*04:01
Racle__3971_ORA_DR	DRB1*13:03,DRB1*07:01,DRB3*01:01,DRB4*01:01,DQA1*02:01-DQB1*02:02,DQA1*02:01-

	DQB1*03:01,DQA1*05:05-DQB1*02:02,DQA1*05:05-DQB1*03:01,DPA1*01:03-DPB1*04:01,DPA1*02:02-DPB1*04:01
Racle__3993	DRB1*07:01,DRB1*15:01,DRB4*01:03,DRB5*01:01,DQA1*01:02-DQB1*02:02,DQA1*01:02-DQB1*06:02,DQA1*02:01-DQB1*02:02,DQA1*02:01-DQB1*06:02,DPA1*01:03-DPB1*04:01,DPA1*01:03-DPB1*17:01,DPA1*02:01-DPB1*04:01,DPA1*02:01-DPB1*17:01
Racle__4001	DRB1*13:01,DRB1*14:01,DRB3*01:01,DRB3*02:02,DQA1*01:03-DQB1*05:03,DQA1*01:03-DQB1*06:03,DQA1*01:04-DQB1*05:03,DQA1*01:04-DQB1*06:03,DPA1*01:03-DPB1*04:01,DPA1*01:03-DPB1*04:02
Racle__4001_DR	DRB1*13:01,DRB1*14:01,DRB3*01:01,DRB3*02:02,DQA1*01:03-DQB1*05:03,DQA1*01:03-DQB1*06:03,DQA1*01:04-DQB1*05:03,DQA1*01:04-DQB1*06:03,DPA1*01:03-DPB1*04:01,DPA1*01:03-DPB1*04:02
Racle__4021	DRB1*11:01,DRB1*04:05,DRB3*02:02,DRB4*01:03,DQA1*03:03-DQB1*02:02,DQA1*03:03-DQB1*03:01,DQA1*05:05-DQB1*02:02,DQA1*05:05-DQB1*03:01,DPA1*01:03-DPB1*03:01,DPA1*01:03-DPB1*10:40
Racle__4021_DQP	DRB1*11:01,DRB1*04:05,DRB3*02:02,DRB4*01:03,DQA1*03:03-DQB1*02:02,DQA1*03:03-DQB1*03:01,DQA1*05:05-DQB1*02:02,DQA1*05:05-DQB1*03:01,DPA1*01:03-DPB1*03:01,DPA1*01:03-DPB1*10:40
Racle__4021_DR	DRB1*11:01,DRB1*04:05,DRB3*02:02,DRB4*01:03,DQA1*03:03-DQB1*02:02,DQA1*03:03-DQB1*03:01,DQA1*05:05-DQB1*02:02,DQA1*05:05-DQB1*03:01,DPA1*01:03-DPB1*03:01,DPA1*01:03-DPB1*10:40
Racle__4037_DC	DRB1*01:01,DQA1*01:01-DQB1*05:01,DPA1*01:03-DPB1*04:01,DPA1*01:03-DPB1*06:01
Racle__4052_BA	DRB1*03:01,DRB1*11:04,DRB3*01:01,DRB3*02:02,DQA1*05:01-DQB1*02:01,DQA1*05:01-DQB1*03:01,DQA1*05:05-DQB1*02:01,DQA1*05:05-DQB1*03:01,DPA1*01:03-DPB1*04:01
Racle__4052_BA_DQP	DRB1*03:01,DRB1*11:04,DRB3*01:01,DRB3*02:02,DQA1*05:01-DQB1*02:01,DQA1*05:01-DQB1*03:01,DQA1*05:05-DQB1*02:01,DQA1*05:05-DQB1*03:01,DPA1*01:03-DPB1*04:01
Racle__4052_BA_DR	DRB1*03:01,DRB1*11:04,DRB3*01:01,DRB3*02:02,DQA1*05:01-DQB1*02:01,DQA1*05:01-DQB1*03:01,DQA1*05:05-DQB1*02:01,DQA1*05:05-DQB1*03:01,DPA1*01:03-DPB1*04:01
Racle__BP455	DRB1*10:01,DRB1*13:01,DRB3*01:01,DQA1*01:05-DQB1*05:01,DQA1*01:05-DQB1*06:03,DQA1*01:10-DQB1*05:01,DQA1*01:10-DQB1*06:03,DPA1*01:03-DPB1*02:01
Racle__CD165	DRB1*11:01,DRB3*02:02,DQA1*05:05-DQB1*03:01,DPA1*01:03-DPB1*04:01,DPA1*01:03-DPB1*04:02
Racle__CD165_DQP	DRB1*11:01,DRB3*02:02,DQA1*05:05-DQB1*03:01,DPA1*01:03-DPB1*04:01,DPA1*01:03-DPB1*04:02
Racle__CD165_DR	DRB1*11:01,DRB3*02:02,DQA1*05:05-DQB1*03:01,DPA1*01:03-DPB1*04:01,DPA1*01:03-DPB1*04:02
Racle__CM647	DRB1*07:01,DRB1*16:01,DRB4*01:03,DRB5*02:02,DQA1*01:02-DQB1*02:02,DQA1*01:02-DQB1*05:02,DQA1*02:01-DQB1*02:02,DQA1*02:01-DQB1*05:02,DPA1*01:03-DPB1*02:01,DPA1*01:03-DPB1*23:01
Racle__CM647_DQP	DRB1*07:01,DRB1*16:01,DRB4*01:03,DRB5*02:02,DQA1*01:02-DQB1*02:02,DQA1*01:02-DQB1*05:02,DQA1*02:01-DQB1*02:02,DQA1*02:01-DQB1*05:02,DPA1*01:03-DPB1*02:01,DPA1*01:03-DPB1*23:01
Racle__CM647_DR	DRB1*07:01,DRB1*16:01,DRB4*01:03,DRB5*02:02,DQA1*01:02-DQB1*02:02,DQA1*01:02-DQB1*05:02,DQA1*02:01-DQB1*02:02,DQA1*02:01-DQB1*05:02,DPA1*01:03-DPB1*02:01,DPA1*01:03-DPB1*23:01
Racle__GD149	DRB1*07:01,DRB1*13:01,DRB3*01:01,DRB4*01:01,DQA1*01:10-DQB1*02:02,DQA1*01:10-DQB1*06:03,DQA1*02:01-DQB1*02:02,DQA1*02:01-DQB1*06:03,DPA1*01:03-DPB1*03:01,DPA1*01:03-DPB1*04:01,DPA1*02:01-DPB1*03:01,DPA1*02:01-DPB1*04:01
Racle__JY	DRB1*04:04,DRB1*13:01,DRB3*01:01,DRB4*01:03,DQA1*01:03-DQB1*03:02,DQA1*01:03-DQB1*06:03,DQA1*03:01-DQB1*03:02,DQA1*03:01-DQB1*06:03,DPA1*01:03-DPB1*02:01,DPA1*01:03-DPB1*04:01
Racle__JY_DR	DRB1*04:04,DRB1*13:01,DRB3*01:01,DRB4*01:03,DQA1*01:03-DQB1*03:02,DQA1*01:03-DQB1*06:03,DQA1*03:01-DQB1*03:02,DQA1*03:01-DQB1*06:03,DPA1*01:03-DPB1*02:01,DPA1*01:03-DPB1*04:01
Racle__PD42	DRB1*01:02,DRB1*15:01,DRB5*01:01,DQA1*01:01-DQB1*05:01,DQA1*01:01-DQB1*06:02,DQA1*01:02-DQB1*05:01,DQA1*01:02-DQB1*06:02,DPA1*01:03-DPB1*04:01,DPA1*01:03-DPB1*05:01,DPA1*02:02-DPB1*04:01,DPA1*02:02-DPB1*05:01

Racle__RA957	DRB1*04:01,DRB1*08:01,DRB4*01:03,DQA1*03:03-DQB1*03:01,DQA1*03:03-DQB1*04:02,DQA1*04:01-DQB1*03:01,DQA1*04:01-DQB1*04:02,DPA1*01:03-DPB1*04:01,DPA1*01:03-DPB1*04:02
Racle__RA957_DQP	DRB1*04:01,DRB1*08:01,DRB4*01:03,DQA1*03:03-DQB1*03:01,DQA1*03:03-DQB1*04:02,DQA1*04:01-DQB1*03:01,DQA1*04:01-DQB1*04:02,DPA1*01:03-DPB1*04:01,DPA1*01:03-DPB1*04:02
Racle__RA957_DR	DRB1*04:01,DRB1*08:01,DRB4*01:03,DQA1*03:03-DQB1*03:01,DQA1*03:03-DQB1*04:02,DQA1*04:01-DQB1*03:01,DQA1*04:01-DQB1*04:02,DPA1*01:03-DPB1*04:01,DPA1*01:03-DPB1*04:02
Racle__TIL1	DRB1*01:01,DRB1*04:08,DRB4*01:03,DQA1*01:01-DQB1*03:01,DQA1*01:01-DQB1*05:01,DQA1*03:03-DQB1*03:01,DQA1*03:03-DQB1*05:01,DPA1*01:03-DPB1*02:01,DPA1*01:03-DPB1*04:01
Racle__TIL3	DRB1*12:01,DRB1*15:01,DRB3*02:02,DRB5*01:01,DQA1*01:02-DQB1*03:01,DQA1*01:02-DQB1*05:02,DQA1*05:05-DQB1*03:01,DQA1*05:05-DQB1*05:02,DPA1*01:03-DPB1*03:01,DPA1*01:03-DPB1*04:01
Ritz__DOHH2_DQ	DRB1*01:01,DRB1*15:01,DRB5*01:01,DQA1*01:01-DQB1*05:01,DQA1*01:02-DQB1*06:02,DQA1*01:02-DQB1*05:01,DQA1*01:01-DQB1*06:02
Ritz__DOHH2_DR	DRB1*01:01,DRB1*15:01,DRB5*01:01,DQA1*01:01-DQB1*05:01,DQA1*01:02-DQB1*06:02,DQA1*01:02-DQB1*05:01,DQA1*01:01-DQB1*06:02
Ritz__Maver_1_DQ	DRB1*01:01,DRB1*13:01,DRB3*02:02,DQA1*01:01-DQB1*05:01,DQA1*01:03-DQB1*06:03,DQA1*01:01-DQB1*06:03,DQA1*01:03-DQB1*05:01
Ritz__Maver_1_DR	DRB1*01:01,DRB1*13:01,DRB3*02:02,DQA1*01:01-DQB1*05:01,DQA1*01:03-DQB1*06:03,DQA1*01:01-DQB1*06:03,DQA1*01:03-DQB1*05:01
Saghar__peptide_0901	DRB1*09:01,DRB4*01:03
Saghar__peptide_1401	DRB1*14:01,DRB3*02:02
Saghar__peptide_1601	DRB1*16:01,DRB5*02:02
Saghar__peptide_HeLa	DRB1*01:02
Scally__DRB1_0401	DRB1*04:01,DRB4*01:01
Scally__DRB1_0402	DRB1*04:02
Scally__DRB1_0404	DRB1*04:04,DRB4*01:01
Sofron__A20	H-2-IAd,H-2-IEd
Sofron__Balb_c_1	H-2-IAd,H-2-IEd
Sofron__Balb_c_2	H-2-IAd,H-2-IEd
Sofron__C57BL_6_1	H-2-IAb
Sofron__C57BL_6_2	H-2-IAb
Ting__T2_DRB1_0405	DRB1*04:05,DRB4*01:01
Wang__LA3	DRB1*03:01,DRB1*15:01,DRB3*01:01,DRB5*01:01
Wang__LA4	DRB1*11:01,DRB1*13:02,DRB3*02:02,DRB3*03:01
Wang__LA5	DRB1*03:01,DRB1*03:05,DRB3*01:01
Wang__LA7	DRB1*04:03,DRB1*15:01,DRB5*01:01
Wang__LA8	DRB1*04:01,DRB1*10:01,DRB4*01:01
Wang__RA2	DRB1*01:01,DRB1*04:01,DRB4*01:01
Wang__RA3	DRB1*01:01,DRB1*04:01,DRB4*01:01

Supplementary table 2: Novel peptide ligand dataset, in the format PEPTIDE 1 CELL_LINE_ID CONTEXT. The data can be found in the external datafile *saghar_peptide_data.xlsx*.

Supplementary table 3: Migration of peptides annotated towards HLA-DQ by the models trained with (w_Saghar) and without (wo_Saghar) the novel data.

Peptides uniquely assigned to HLA-DQ in w_Saghar method	**Distribution of peptide annotations in wo_Saghar method**		
	HLA-DP	**HLA-DR**	**Trash**
9309	1816	4688	2805
Peptides uniquely assigned to HLA-DQ in wo_Saghar method	**Distribution of peptide annotations in w_Saghar method**		
	HLA-DP	**HLA-DR**	**Trash**
4316	609	2629	1078

1049 **Supplementary table 4: Overview of peptides assigned to DQ molecules in the methods with (w_Saghar) and**
1050 **without (wo_Saghar) the novel data.** Trash peptides with percentile rank greater than 20 are not included in the
1051 metrics. A bold value indicates either a higher average peptide count or a lower mean/median percentile rank in a
1052 given method.
1053

	Average number of peptides per dataset		Average of per-dataset mean percentile rank		Median of per-dataset median percentile rank	
Molecule	**w_Saghar**	**wo_Saghar**	**w_Saghar**	**wo_Saghar**	**w_Saghar**	**wo_Saghar**
HLA-DQA1*01:01-DQB1*02:01	6.00	**7.50**	**3.2818**	3.7402	**0.6713**	0.8226
HLA-DQA1*01:01-DQB1*03:01	20.00	**170.00**	**0.3084**	1.8631	**0.0086**	0.4087
HLA-DQA1*01:01-DQB1*03:03	27.00	**58.00**	**0.4281**	0.5240	**0.0078**	0.0086
HLA-DQA1*01:01-DQB1*05:01	**209.53**	155.06	2.6547	**1.1562**	1.1783	**0.1096**
HLA-DQA1*01:01-DQB1*06:02	**30.50**	27.67	1.1216	**0.9356**	**0.2011**	0.2064
HLA-DQA1*01:01-DQB1*06:03	26.40	**59.20**	**1.2573**	2.6273	**0.1503**	2.1822
HLA-DQA1*01:02-DQB1*02:02	13.00	**28.75**	**0.1723**	1.3248	**0.0073**	0.0094
HLA-DQA1*01:02-DQB1*03:01	53.00	**99.00**	**0.3111**	1.5251	**0.0083**	0.0552
HLA-DQA1*01:02-DQB1*03:02	6.50	**8.50**	**0.3849**	0.8472	**0.0073**	0.0078
HLA-DQA1*01:02-DQB1*05:01	27.33	**43.33**	2.2276	**0.8075**	0.1011	**0.0092**
HLA-DQA1*01:02-DQB1*05:02	**512.20**	368.00	2.7410	**1.1782**	0.6769	**0.0513**
HLA-DQA1*01:02-DQB1*06:02	550.88	**551.88**	4.1209	**3.8584**	1.9511	**1.5487**
HLA-DQA1*01:02-DQB1*06:04	**1548.50**	1520.00	**1.8068**	1.9438	**0.3963**	0.4895
HLA-DQA1*01:03-DQB1*03:02	23.50	**54.50**	**0.3737**	0.9327	**0.0071**	0.0091
HLA-DQA1*01:03-DQB1*05:01	6.60	**12.80**	0.6552	**0.3573**	**0.0140**	0.0165
HLA-DQA1*01:03-DQB1*05:03	**2.00**	1.50	4.2220	**0.0102**	4.2220	**0.0102**
HLA-DQA1*01:03-DQB1*06:03	**353.10**	325.60	**2.6588**	3.0594	**0.5745**	0.5782
HLA-DQA1*01:04-DQB1*05:03	**549.00**	406.33	2.8193	**0.7154**	**1.7952**	0.2739
HLA-DQA1*01:04-DQB1*06:03	3.00	**3.50**	**3.2792**	3.5277	4.1573	**2.3288**
HLA-DQA1*01:05-DQB1*05:01	**89.00**	27.00	2.5292	**1.4787**	1.2150	**0.0631**
HLA-DQA1*01:05-DQB1*06:03	27.00	**51.00**	**0.6273**	0.9981	**0.0100**	0.0225
HLA-DQA1*01:10-DQB1*02:02	6.00	**32.00**	**0.0063**	0.0663	**0.0067**	0.0073
HLA-DQA1*01:10-DQB1*05:01	17.00	**22.00**	**0.0983**	0.9877	**0.0077**	0.0085
HLA-DQA1*01:10-DQB1*06:03	**205.00**	189.00	**1.9616**	1.9742	0.5409	**0.4139**

HLA-DQA1*02:01-DQB1*02:01	**75.67**	73.33	**2.2314**	2.3259	0.5515	**0.3520**
HLA-DQA1*02:01-DQB1*02:02	1188.91	**1207.82**	3.4357	**2.9958**	1.1275	**1.1813**
HLA-DQA1*02:01-DQB1*03:01	8.00	**10.50**	6.1621	**4.9487**	**2.2676**	2.6416
HLA-DQA1*02:01-DQB1*03:03	**868.00**	711.00	3.8598	**2.8138**	2.0423	**0.9332**
HLA-DQA1*02:01-DQB1*05:01	11.00	**24.00**	**0.0094**	1.5804	**0.0060**	0.0080
HLA-DQA1*02:01-DQB1*05:02	**18.33**	15.67	**0.0088**	2.0617	**0.0059**	0.0083
HLA-DQA1*02:01-DQB1*06:02	6.00	**7.00**	1.0585	**0.0980**	0.0355	**0.0091**
HLA-DQA1*02:01-DQB1*06:03	15.00	15.00	**0.0088**	0.2958	0.0085	**0.0072**
HLA-DQA1*03:01-DQB1*02:01	**14.67**	14.33	3.0440	**2.0955**	**0.0953**	0.9899
HLA-DQA1*03:01-DQB1*03:01	**54.67**	16.83	3.5246	**0.7732**	1.1628	**0.0092**
HLA-DQA1*03:01-DQB1*03:02	**152.86**	92.64	4.2735	**1.5354**	2.0231	**0.1016**
HLA-DQA1*03:01-DQB1*06:02	**4.00**	1.00	2.3313	**0.4498**	**0.2132**	0.4498
HLA-DQA1*03:01-DQB1*06:03	8.00	**10.00**	0.6198	**0.0115**	0.0270	**0.0088**
HLA-DQA1*03:02-DQB1*03:03	**1565.00**	1003.00	3.3282	**2.6386**	1.4368	**0.6301**
HLA-DQA1*03:03-DQB1*02:02	**48.33**	15.00	0.8371	**0.1817**	**0.0096**	0.0109
HLA-DQA1*03:03-DQB1*03:01	**593.25**	389.50	3.0677	**1.0865**	0.8015	**0.0512**
HLA-DQA1*03:03-DQB1*04:02	**82.00**	17.00	**0.8113**	1.2414	**0.0109**	0.0204
HLA-DQA1*03:03-DQB1*05:01	**9.00**	4.00	**0.0143**	0.0253	**0.0085**	0.0258
HLA-DQA1*04:01-DQB1*03:01	96.67	**371.00**	**1.4585**	3.5739	**0.0179**	1.5131
HLA-DQA1*04:01-DQB1*04:02	**967.60**	801.80	3.0511	**2.3695**	1.4733	**0.5541**
HLA-DQA1*05:01-DQB1*02:01	344.00	**347.79**	**2.2603**	2.6852	**0.2518**	0.3707
HLA-DQA1*05:01-DQB1*03:01	1008.50	1008.50	4.6531	**4.3624**	1.7700	**1.6834**
HLA-DQA1*05:01-DQB1*03:02	19.67	**22.00**	3.5080	**2.4423**	**0.2787**	0.5770
HLA-DQA1*05:01-DQB1*05:01	2.00	**4.00**	**0.0071**	0.0238	**0.0070**	0.0082
HLA-DQA1*05:05-DQB1*02:02	**64.00**	62.40	2.4021	**2.1639**	**0.1911**	0.3171
HLA-DQA1*05:05-DQB1*03:01	577.55	**594.90**	**3.3196**	3.8926	**1.4065**	1.8265
HLA-DQA1*05:05-DQB1*03:02	18.67	**25.33**	**1.2711**	1.5989	0.0884	**0.0495**
HLA-DQA1*05:05-DQB1*05:02	**24.00**	9.00	0.0093	**0.0068**	**0.0064**	0.0071

Supplementary table 5: Overview of consistency analysis in the methods with (w_Saghar) and without (wo_Saghar) the novel data. The molecules are sorted in descending order by the difference in mean consistency. Further, the metrics are calculated on the peptide sets used in the consistency analysis, with the union of identified trash peptides removed. As such, the metrics regarding differences in percentile ranks may not correspond one-to-one with the values in supplementary table 4.

Molecules	Difference in mean consistency (w_Saghar - wo_Saghar)	Number of cell lines with at least 20 peptides in both methods	Number of cell lines with larger peptide count in w_Saghar	Number of cell lines with lower mean %rank in w_Saghar	Fraction of cell lines with either larger peptide count or lower mean %rank in w_Saghar
HLA-DQA1*03:01-DQB1*03:02	**0.148**	**6**	**6**	**1**	**1.000**
HLA-DQA1*03:01-DQB1*03:01	**0.147**	**2**	**2**	**0**	**1.000**
HLA-DQA1*03:03-DQB1*03:01	**0.119**	**5**	**5**	**1**	**1.000**
HLA-DQA1*01:01-DQB1*05:01	**0.079**	**10**	**10**	**3**	**1.000**
HLA-DQA1*04:01-DQB1*04:02	**0.039**	**5**	**3**	**2**	**0.600**
HLA-DQA1*01:02-DQB1*05:02	**0.037**	**5**	**5**	**1**	**1.000**
HLA-DQA1*02:01-DQB1*03:03	**0.035**	**2**	**2**	**1**	**1.000**
HLA-DQA1*01:10-DQB1*06:03	**0.034**	**2**	**2**	**1**	**1.000**
HLA-DQA1*05:05-DQB1*03:01	**0.027**	**16**	**2**	**8**	**0.625**
HLA-DQA1*01:02-DQB1*06:02	**0.020**	**7**	**3**	**1**	**0.429**
HLA-DQA1*02:01-DQB1*02:01	**0.017**	**3**	**2**	**1**	**0.667**
HLA-DQA1*05:01-DQB1*02:01	**0.016**	**12**	**4**	**9**	**0.917**
HLA-DQA1*05:05-DQB1*02:02	**0.014**	**3**	**0**	**2**	**0.667**
HLA-DQA1*02:01-DQB1*02:02	**0.010**	**9**	**1**	**8**	**1.000**
HLA-DQA1*05:05-DQB1*03:02	**0.005**	**2**	**1**	**1**	**1.000**
HLA-DQA1*05:01-DQB1*03:01	**0.002**	**4**	**3**	**0**	**0.750**
HLA-DQA1*01:02-DQB1*06:04	-0.002	2	1	2	1.000
HLA-DQA1*01:03-DQB1*03:02	-0.008	2	0	2	1.000
HLA-DQA1*01:03-DQB1*06:03	-0.009	7	5	4	0.857
HLA-DQA1*01:01-DQB1*06:03	-0.027	2	0	2	1.000
HLA-DQA1*04:01-DQB1*03:01	-0.031	3	0	3	1.000

Supplementary table 6: Overview of DQ-heterozygous datasets used in the cis vs trans-only DQ analysis, along with their DQ HLA typing. Molecules marked in red are trans-only heterodimers. Molecules in bold are part of the DQ-SA training data.

Dataset	DQ heterodimers			
Racle__3808_HMC	DQA1*02:01-DQB1*02:01	**DQA1*02:01-DQB1*02:02**	**DQA1*05:01-DQB1*02:01**	DQA1*05:01-DQB1*02:02
Racle__3830NJF	DQA1*03:01-DQB1*03:01	**DQA1*03:01-DQB1*03:02**	**DQA1*05:05-DQB1*03:01**	DQA1*05:05-DQB1*03:02
Racle__3830_NJF_DQP	DQA1*03:01-DQB1*03:01	**DQA1*03:01-DQB1*03:02**	**DQA1*05:05-DQB1*03:01**	DQA1*05:05-DQB1*03:02
Racle__3865DM	DQA1*01:01-DQB1*03:03	**DQA1*01:01-DQB1*05:01**	**DQA1*02:01-DQB1*03:03**	DQA1*02:01-DQB1*05:01
Racle__3869_GA	DQA1*03:01-DQB1*03:01	**DQA1*03:01-DQB1*03:02**	**DQA1*05:05-DQB1*03:01**	DQA1*05:05-DQB1*03:02
Racle__3869_GA_DQP	DQA1*03:01-DQB1*03:01	**DQA1*03:01-DQB1*03:02**	**DQA1*05:05-DQB1*03:01**	DQA1*05:05-DQB1*03:02
Racle__3912BAM	DQA1*03:01-DQB1*02:01	**DQA1*03:01-DQB1*03:02**	**DQA1*05:01-DQB1*02:01**	DQA1*05:01-DQB1*03:02
Racle__3912_BAM_DR	DQA1*03:01-DQB1*02:01	**DQA1*03:01-DQB1*03:02**	**DQA1*05:01-DQB1*02:01**	DQA1*05:01-DQB1*03:02
Racle__3947_GA	**DQA1*01:01-DQB1*05:01**	DQA1*01:01-DQB1*06:03	DQA1*01:03-DQB1*05:01	**DQA1*01:03-DQB1*06:03**
Racle__4021	DQA1*03:03-DQB1*02:02	**DQA1*03:03-DQB1*03:01**	DQA1*05:05-DQB1*02:02	**DQA1*05:05-DQB1*03:01**
Racle__4021_DQP	DQA1*03:03-DQB1*02:02	**DQA1*03:03-DQB1*03:01**	DQA1*05:05-DQB1*02:02	**DQA1*05:05-DQB1*03:01**
Racle__4052_BA	**DQA1*05:01-DQB1*02:01**	DQA1*05:01-DQB1*03:01	DQA1*05:05-DQB1*02:01	**DQA1*05:05-DQB1*03:01**
Racle__4052_BA_DQP	**DQA1*05:01-DQB1*02:01**	DQA1*05:01-DQB1*03:01	DQA1*05:05-DQB1*02:01	**DQA1*05:05-DQB1*03:01**
Racle__BP455	DQA1*01:05-DQB1*05:01	DQA1*01:05-DQB1*06:03	DQA1*01:10-DQB1*05:01	DQA1*01:10-DQB1*06:03
Racle__CM647	DQA1*01:02-DQB1*02:02	**DQA1*01:02-DQB1*05:02**	**DQA1*02:01-DQB1*02:02**	DQA1*02:01-DQB1*05:02
Racle__CM647_DQP	DQA1*01:02-DQB1*02:02	**DQA1*01:02-DQB1*05:02**	**DQA1*02:01-DQB1*02:02**	DQA1*02:01-DQB1*05:02
Racle__CM647_DR	DQA1*01:02-DQB1*02:02	**DQA1*01:02-DQB1*05:02**	**DQA1*02:01-DQB1*02:02**	DQA1*02:01-DQB1*05:02
Racle__GD149	DQA1*01:10-DQB1*02:02	DQA1*01:10-DQB1*06:03	**DQA1*02:01-DQB1*02:02**	DQA1*02:01-DQB1*06:03
Racle__JY	DQA1*01:03-DQB1*03:02	**DQA1*01:03-DQB1*06:03**	**DQA1*03:01-DQB1*03:02**	DQA1*03:01-DQB1*06:03
Racle__JY_DR	DQA1*01:03-DQB1*03:02	**DQA1*01:03-DQB1*06:03**	**DQA1*03:01-DQB1*03:02**	DQA1*03:01-DQB1*06:03
Racle__PD42	**DQA1*01:01-DQB1*05:01**	DQA1*01:01-DQB1*06:02	DQA1*01:02-DQB1*05:01	**DQA1*01:02-DQB1*06:02**
Racle__RA957	**DQA1*03:03-DQB1*03:01**	DQA1*03:03-DQB1*04:02	DQA1*04:01-DQB1*03:01	**DQA1*04:01-DQB1*04:02**
Racle__RA957_DQP	**DQA1*03:03-DQB1*03:01**	DQA1*03:03-DQB1*04:02	DQA1*04:01-DQB1*03:01	**DQA1*04:01-DQB1*04:02**
Racle__RA957_DR	**DQA1*03:03-DQB1*03:01**	DQA1*03:03-DQB1*04:02	DQA1*04:01-DQB1*03:01	**DQA1*04:01-DQB1*04:02**
Racle__TIL1	DQA1*01:01-DQB1*03:01	**DQA1*01:01-DQB1*05:01**	**DQA1*03:03-DQB1*03:01**	DQA1*03:03-DQB1*05:01
Racle__TIL3	DQA1*01:02-DQB1*03:01	**DQA1*01:02-DQB1*05:02**	**DQA1*05:05-DQB1*03:01**	DQA1*05:05-DQB1*05:02
Ritz__DOHH2_DQ	**DQA1*01:01-DQB1*05:01**	**DQA1*01:02-DQB1*06:02**	DQA1*01:02-DQB1*05:01	DQA1*01:01-DQB1*06:02
Ritz__Maver_1_DQ	**DQA1*01:01-DQB1*05:01**	**DQA1*01:03-DQB1*06:03**	DQA1*01:01-DQB1*06:03	DQA1*01:03-DQB1*05:01

Supplementary table 7: DQ molecules covered by the method including the novel data. The highlighted molecules are covered by a peptide count of at least 100, while the remaining molecules have a distance of at most 0.025 to one of the highlighted molecules.

HLA-DQA1*01:01-DQB1*05:01	HLA-DQA1*01:01-DQB1*05:02	HLA-DQA1*03:01-DQB1*02:02	HLA-DQA1*05:01-DQB1*03:19
HLA-DQA1*01:01-DQB1*06:03	HLA-DQA1*01:01-DQB1*05:03	HLA-DQA1*03:01-DQB1*03:03	HLA-DQA1*05:01-DQB1*03:22
HLA-DQA1*01:02-DQB1*05:02	HLA-DQA1*01:01-DQB1*06:02	HLA-DQA1*03:01-DQB1*03:19	HLA-DQA1*05:01-DQB1*03:62
HLA-DQA1*01:02-DQB1*06:02	HLA-DQA1*01:01-DQB1*06:04	HLA-DQA1*03:01-DQB1*03:22	HLA-DQA1*05:02-DQB1*02:01
HLA-DQA1*01:02-DQB1*06:04	HLA-DQA1*01:02-DQB1*05:01	HLA-DQA1*03:01-DQB1*03:62	HLA-DQA1*05:02-DQB1*02:02
HLA-DQA1*01:03-DQB1*06:03	HLA-DQA1*01:02-DQB1*05:03	HLA-DQA1*03:01-DQB1*03:87	HLA-DQA1*05:02-DQB1*03:01
HLA-DQA1*01:04-DQB1*05:03	HLA-DQA1*01:02-DQB1*05:46	HLA-DQA1*03:01-DQB1*04:01	HLA-DQA1*05:02-DQB1*03:02
HLA-DQA1*01:10-DQB1*06:03	HLA-DQA1*01:02-DQB1*06:03	HLA-DQA1*03:01-DQB1*04:02	HLA-DQA1*05:03-DQB1*02:01
HLA-DQA1*02:01-DQB1*02:01	HLA-DQA1*01:03-DQB1*05:02	HLA-DQA1*03:02-DQB1*02:01	HLA-DQA1*05:03-DQB1*02:02
HLA-DQA1*02:01-DQB1*02:02	HLA-DQA1*01:03-DQB1*06:02	HLA-DQA1*03:02-DQB1*02:02	HLA-DQA1*05:03-DQB1*03:01
HLA-DQA1*02:01-DQB1*03:03	HLA-DQA1*01:03-DQB1*06:04	HLA-DQA1*03:02-DQB1*03:01	HLA-DQA1*05:03-DQB1*03:02
HLA-DQA1*03:01-DQB1*03:01	HLA-DQA1*01:04-DQB1*05:01	HLA-DQA1*03:02-DQB1*03:02	HLA-DQA1*05:03-DQB1*03:22
HLA-DQA1*03:01-DQB1*03:02	HLA-DQA1*01:04-DQB1*05:02	HLA-DQA1*03:02-DQB1*03:22	HLA-DQA1*05:05-DQB1*02:01
HLA-DQA1*03:02-DQB1*03:03	HLA-DQA1*01:04-DQB1*06:02	HLA-DQA1*03:02-DQB1*04:01	HLA-DQA1*05:05-DQB1*03:22
HLA-DQA1*03:03-DQB1*02:02	HLA-DQA1*01:04-DQB1*06:03	HLA-DQA1*03:02-DQB1*04:02	HLA-DQA1*05:06-DQB1*03:01
HLA-DQA1*03:03-DQB1*03:01	HLA-DQA1*01:04-DQB1*06:04	HLA-DQA1*03:03-DQB1*02:01	HLA-DQA1*05:06-DQB1*03:02
HLA-DQA1*03:03-DQB1*04:02	HLA-DQA1*01:05-DQB1*05:01	HLA-DQA1*03:03-DQB1*03:02	HLA-DQA1*05:08-DQB1*02:01
HLA-DQA1*04:01-DQB1*03:01	HLA-DQA1*01:05-DQB1*05:02	HLA-DQA1*03:03-DQB1*03:03	HLA-DQA1*05:08-DQB1*03:01
HLA-DQA1*04:01-DQB1*04:02	HLA-DQA1*01:05-DQB1*05:03	HLA-DQA1*03:03-DQB1*03:22	HLA-DQA1*05:08-DQB1*03:02
HLA-DQA1*05:01-DQB1*02:01	HLA-DQA1*01:05-DQB1*06:02	HLA-DQA1*03:03-DQB1*04:01	HLA-DQA1*06:01-DQB1*03:01
HLA-DQA1*05:01-DQB1*03:01	HLA-DQA1*01:05-DQB1*06:03	HLA-DQA1*04:01-DQB1*03:22	HLA-DQA1*06:01-DQB1*03:22
HLA-DQA1*05:05-DQB1*02:02	HLA-DQA1*01:05-DQB1*06:04	HLA-DQA1*04:01-DQB1*04:01	HLA-DQA1*06:01-DQB1*04:01
HLA-DQA1*05:05-DQB1*03:01	HLA-DQA1*02:01-DQB1*03:87	HLA-DQA1*05:01-DQB1*02:02	HLA-DQA1*06:01-DQB1*04:02
HLA-DQA1*05:05-DQB1*03:02	HLA-DQA1*03:01-DQB1*02:01	HLA-DQA1*05:01-DQB1*03:02	

Supplementary table 8: Prevalent DQ molecules with distance greater than 0.025 to molecules covered by the method including the novel data.

HLA-DQA1*01:01-DQB1*05:04	HLA-DQA1*01:04-DQB1*06:09	HLA-DQA1*04:01-DQB1*02:01	HLA-DQA1*05:03-DQB1*03:03
HLA-DQA1*01:01-DQB1*06:01	HLA-DQA1*01:05-DQB1*06:01	HLA-DQA1*04:01-DQB1*02:02	HLA-DQA1*05:03-DQB1*03:04
HLA-DQA1*01:01-DQB1*06:05	HLA-DQA1*02:01-DQB1*03:01	HLA-DQA1*04:01-DQB1*03:02	HLA-DQA1*05:03-DQB1*03:05
HLA-DQA1*01:01-DQB1*06:09	HLA-DQA1*02:01-DQB1*03:02	HLA-DQA1*04:01-DQB1*03:03	HLA-DQA1*05:03-DQB1*04:01
HLA-DQA1*01:02-DQB1*05:04	HLA-DQA1*02:01-DQB1*03:04	HLA-DQA1*04:01-DQB1*03:04	HLA-DQA1*05:03-DQB1*04:02
HLA-DQA1*01:02-DQB1*06:01	HLA-DQA1*02:01-DQB1*03:05	HLA-DQA1*04:01-DQB1*03:05	HLA-DQA1*05:05-DQB1*03:03
HLA-DQA1*01:02-DQB1*06:05	HLA-DQA1*02:01-DQB1*03:19	HLA-DQA1*05:01-DQB1*02:03	HLA-DQA1*05:05-DQB1*03:04
HLA-DQA1*01:02-DQB1*06:09	HLA-DQA1*02:01-DQB1*03:22	HLA-DQA1*05:01-DQB1*03:03	HLA-DQA1*05:05-DQB1*03:05
HLA-DQA1*01:03-DQB1*05:01	HLA-DQA1*02:01-DQB1*03:62	HLA-DQA1*05:01-DQB1*03:04	HLA-DQA1*05:05-DQB1*04:01
HLA-DQA1*01:03-DQB1*05:03	HLA-DQA1*02:01-DQB1*04:01	HLA-DQA1*05:01-DQB1*03:05	HLA-DQA1*05:05-DQB1*04:02
HLA-DQA1*01:03-DQB1*05:04	HLA-DQA1*02:01-DQB1*04:02	HLA-DQA1*05:01-DQB1*03:87	HLA-DQA1*05:08-DQB1*03:03
HLA-DQA1*01:03-DQB1*06:01	HLA-DQA1*03:01-DQB1*03:04	HLA-DQA1*05:01-DQB1*04:01	HLA-DQA1*06:01-DQB1*02:01
HLA-DQA1*01:03-DQB1*06:05	HLA-DQA1*03:01-DQB1*03:05	HLA-DQA1*05:01-DQB1*04:02	HLA-DQA1*06:01-DQB1*02:02
HLA-DQA1*01:03-DQB1*06:09	HLA-DQA1*03:02-DQB1*03:04	HLA-DQA1*05:02-DQB1*03:03	HLA-DQA1*06:01-DQB1*03:02
HLA-DQA1*01:04-DQB1*06:01	HLA-DQA1*03:02-DQB1*03:05	HLA-DQA1*05:02-DQB1*04:02	HLA-DQA1*06:01-DQB1*03:03

Supplementary table 9: Overview of donor cell lines and their HLA typing in the benchmark data from Marcu et al. 2021. For the donor Donor_BD_ZH14, the HLA typing was originally listed as having five DQ molecules. As four of these molecules shared two α- and two β-chains, the erroneous extra molecule was found to be DQA1*01:02-DQB1*02:01. This could be a misspelling of DPA1*01:02-DPB1*02:01, however, DPA1*01:02 has been removed from the IMGT/HLA database due to having an erroneous sequence (https://www.ebi.ac.uk/ipd/imgt/hla/alleles/allele/?accession=HLA00498). As such, we decided to delete DQA1*01:02-DQB1*02:01 from the HLA typing of this donor.

Donor_16_113	DRB1*04:01,DRB1*07:01,DQA1*01:01-DQB1*03:01,DQA1*01:01-DQB1*03:03
Donor_BD_ZH01	DRB1*07:01,DRB1*11:01,DRB3*02:02,DRB4*01:01,DQA1*02:01-DQB1*02:02,DQA1*05:01-DQB1*02:02,DPA1*01:03-DPB1*02:01,DPA1*01:03-DPB1*19:01
Donor_BD_ZH02	DRB1*04:01,DRB4*01:01,DQA1*03:01-DQB1*03:01,DQA1*03:02-DQB1*03:01,DPA1*01:03-DPB1*04:01,DPA1*01:03-DPB1*04:02
Donor_BD_ZH03	DRB1*07:01,DRB1*11:03,DRB3*02:02,DRB4*01:01,DQA1*02:01-DQB1*02:02,DQA1*02:01-DQB1*03:01,DQA1*05:05-DQB1*02:02,DQA1*05:05-DQB1*03:01,DPA1*01:03-DPB1*03:01,DPA1*01:03-DPB1*04:01
Donor_BD_ZH04	DRB1*07:01,DRB1*13:01,DRB3*01:01,DRB4*01:01,DQA1*01:03-DQB1*02:02,DQA1*01:03-DQB1*06:03,DQA1*02:01-DQB1*02:02,DQA1*02:01-DQB1*06:03,DPA1*01:03-DPB1*03:01,DPA1*01:03-DPB1*04:01,DPA1*02:02-DPB1*03:01,DPA1*02:02-DPB1*04:01
Donor_BD_ZH05	DRB1*11:01,DRB1*14:54,DRB3*02:02,DQA1*01:01-DQB1*03:01,DQA1*01:01-DQB1*05:03,DQA1*05:05-DQB1*03:01,DQA1*05:05-DQB1*05:03,DPA1*01:03-DPB1*04:01
Donor_BD_ZH06	DRB1*08:01,DRB1*13:03,DRB3*01:01,DQA1*04:01-DQB1*03:01,DQA1*04:01-DQB1*04:02,DQA1*05:05-DQB1*03:01,DQA1*05:05-DQB1*04:02,DPA1*01:03-DPB1*04:01,DPA1*01:03-DPB1*04:02
Donor_BD_ZH07	DRB1*04:01,DRB1*15:01,DRB4*01:01,DRB5*01:01,DQA1*01:02-DQB1*03:01,DQA1*01:02-DQB1*06:02,DQA1*03:01-DQB1*03:01,DQA1*03:01-DQB1*06:02,DPA1*01:03-DPB1*04:02,DPA1*01:03-DPB1*05:01
Donor_BD_ZH08	DRB1*13:03,DRB1*14:01,DQA1*05:05-DQB1*03:01
Donor_BD_ZH09	DRB1*07:01,DRB4*01:03,DQA1*02:01-DQB1*02:02,DPA1*01:03-DPB1*03:01,DPA1*01:03-DPB1*04:02
Donor_BD_ZH11	DRB1*07:01,DRB1*13:02,DRB3*03:01,DRB4*01:03,DQA1*01:02-DQB1*03:03,DQA1*01:02-DQB1*06:04,DQA1*02:01-DQB1*03:03,DQA1*02:01-DQB1*06:04,DPA1*01:03-DPB1*03:01,DPA1*01:03-DPB1*04:01
Donor_BD_ZH12	DRB1*01:01,DRB1*12:01,DRB3*02:02,DQA1*01:01-DQB1*03:01,DQA1*01:01-DQB1*05:01,DQA1*05:05-DQB1*03:01,DQA1*05:05-DQB1*05:01,DPA1*01:03-DPB1*02:01,DPA1*01:03-DPB1*09:01,DPA1*02:01-DPB1*02:01,DPA1*02:01-DPB1*09:01
Donor_BD_ZH13	DRB1*10:01,DRB1*15:01,DRB5*01:01,DQA1*01:01-DQB1*05:01,DQA1*01:01-DQB1*06:02,DQA1*01:02-DQB1*05:01,DQA1*01:02-DQB1*06:02,DPA1*01:03-DPB1*02:01,DPA1*01:03-DPB1*04:02
Donor_BD_ZH14	DRB1*04:01,DRB1*13:03,DRB3*01:01,DRB4*01:03,DQA1*03:02-DQB1*03:01,DQA1*03:02-DQB1*03:02,DQA1*05:05-DQB1*03:01,DQA1*05:05-DQB1*03:02,DPA1*01:03-DPB1*02:01
Donor_BD_ZH15	DRB1*03:01,DRB1*11:01,DRB3*01:01,DRB3*02:02,DQA1*05:01-DQB1*02:01,DQA1*05:01-DQB1*03:01,DPA1*01:03-DPB1*01:01,DPA1*01:03-DPB1*03:01,DPA1*02:01-DPB1*01:01,DPA1*02:01-DPB1*03:01
Donor_BD_ZH16	DRB1*03:01,DRB1*04:05,DQA1*03:02-DQB1*02:01,DQA1*03:02-DQB1*02:02,DQA1*05:01-DQB1*02:01,DQA1*05:01-DQB1*02:02
Donor_BD_ZH17	DRB1*14:54,DRB1*15:01,DRB3*02:02,DRB5*01:01,DQA1*01:01-DQB1*05:03,DQA1*01:01-DQB1*06:02,DQA1*01:02-DQB1*05:03,DQA1*01:02-DQB1*06:02,DPA1*01:03-DPB1*02:01